applied sciences

MDPI

Review

The Importance of Multidisciplinary Analytical Strategies to Solve Identification and Characterization Challenges in Gemology: The Example of the "Green Stones"

Maya Musa [1,2]

[1] Department of Physics "Giuseppe Occhialini", University of Milan Bicocca, 20126 Milan, Italy; maya.musa@unimib.it
[2] Department of Earth and Environmental Sciences (DISAT), University of Milan Bicocca, 20126 Milan, Italy

Featured Application: Based on the data and analytical methodologies reported here, this review can be used as a reference for Green Stones identification and characterization protocols. Moreover, due to the multidisciplinary approach discussed, it can also be considered as an example useful for similar applications.

Abstract: The present review aims to discuss the importance of a multidisciplinary approach in cultural heritage and archaeometry investigations. The analytical methods used to identify and characterize "Green Stones" are discussed as an example. In the present paper, the term Green Stones is applied but not limited to jade materials, which have considerable importance in cultural heritage studies. In fact, archaeological samples made in Green Stones have been discovered worldwide, with many dating back to the Neolithic Age. Moreover, these materials represent an interesting analytical challenge, starting with their nomenclature and, in most cases, the nature of their polycrystalline samples and their heterogeneity. Indeed, after a brief introduction about the advantages of the non-destructive analytical techniques commonly used for gemstones and cultural heritage samples analyses, the limits of the same have been discussed on the basis of Green Stones applicability. Finally, a multidisciplinary methodology for Green Stones identification and full characterization, which considers materials' heterogeneity and information, has been proposed and based on different references.

Keywords: multidisciplinary approach; identification; characterization; green stones; jade; jadeite; nephrite; Fei Cui; maw-sit-sit

Citation: Musa, M. The Importance of Multidisciplinary Analytical Strategies to Solve Identification and Characterization Challenges in Gemology: The Example of the "Green Stones". *Appl. Sci.* **2022**, *12*, 7168. https://doi.org/10.3390/app12147168

Academic Editor: Yosoon Choi

Received: 28 May 2022
Accepted: 14 July 2022
Published: 16 July 2022

1. Introduction

The "multidisciplinary approach" has become very popular in several scientific fields in recent decades [1–5]. However, what do we mean by the term "multidisciplinary"? The definition means "across several fields of study" [6]. For our purposes, it can be applied to at least two different levels: The first one is when experts from various fields of disciplines are involved in studying a problem that can only be solved by their combined efforts. The second one is when an analytical problem can be solved only by applying different diagnostic techniques and combining the results in a typical, so-called multidisciplinary protocol. In many cases, those two approaches are strictly correlated.

More generally, it is possible to assert that a multidisciplinary approach must be applied every time the object of study presents cross scientific peculiarities. For this reason, the interaction, crossing, and overlapping of scientific fields, apparently very far from each other, is not a surprise if the focus is on cultural heritage.

An example of this concept is found in Pasquarella [7], where the authors demonstrated the importance of the multidisciplinary approach, combining biological knowledge and the methodology for aerosol particles characterization in relation to monitoring and conserving

the Palatina historical library in Parma. On the other hand, archaeometry shows an intrinsic, strong multidisciplinary characteristic, due to the typical overlapping of many analytical techniques required for this type of study. In Cardoso [8] study of the mortars from the town of Ammaia (Lusitania, Portugal) has been performed by crossing information acquired by several analytical techniques: stereomicroscopy, X-ray diffraction, thermal analysis, and scanning electron microscopy coupled with energy dispersive X-ray spectroscopy. By these cited experiences plus others [9–18], it is possible to highlight that cultural heritage conservation studies require multidisciplinary approaches to answer the interdisciplinary nature of the problems that must be solved.

And what about the diagnostic issues?

In this scenario, it is interesting to note that archaeometry, by Wagner's (2007) [19] definition, designates the development and application of natural scientific methods in order to contribute to the solution of cultural–historical questions. By this acceptation, for Reindel and Wagner (2009) [20], archaeometry becomes the interface between natural and cultural heritage sciences. On the basis of these considerations, archaeometry shows an intrinsic and significant multidisciplinary component.

In Figure 1, a scheme showing the interdisciplinary aspects of archaeometry for archaeological samples identification is reported.

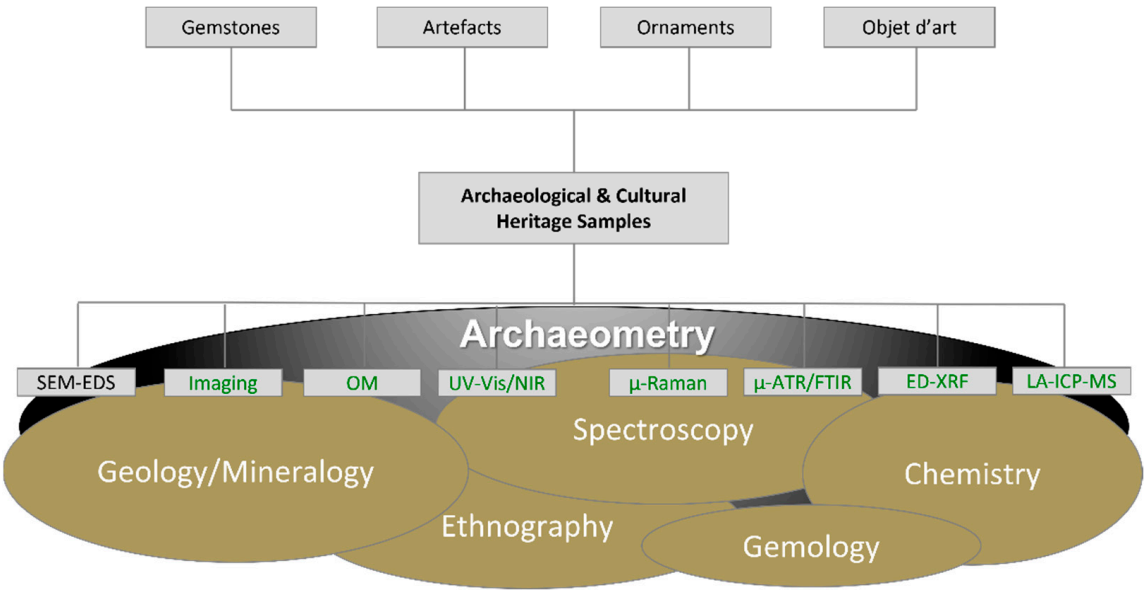

Figure 1. Archaeometry requires a multidisciplinary approach to characterize archaeological and cultural heritage samples. Gemstones, artefacts, ornaments, and objets d'art, with several exceptions, belong to archaeological and cultural heritage samples. To identify and characterize these type of samples, in an archaeometric context, the contributions of different expertise are required, including geologists, mineralogists, etc. Moreover, many analytical techniques are necessary. The acronyms correspond to: SEM-EDS: Scanning Electron Microscopy with Energy Dispersive Spectroscopy; OM: Optical Microscopy; UV-Vis/NIR: Ultraviolet-Visible/Near-InfraRed spectroscopy; μ-Raman: micro-Raman Spectroscopy; μ-ATR/FTIR: micro-Attenuated Total Reflection/Fourier Transform InfraRed Spectroscopy; ED-XRF: Energy Dispersive X-ray Fluorescence; LA-ICP-MS: Laser Ablation Inductively Coupled Plasma Mass Spectrometry. Imaging techniques: the term "imaging" is commonly used for diagnostics-per-image systems, which typically include multispectral observation (i.e., imaging by fluorescence reaction, Wood lamp, etc.). It is interesting to note that all techniques reported by the green color in the gray boxes are typically applied in scientific gemology.

It is interesting to note that both levels of multidisciplinary approaches, namely multidisciplinary diagnostic protocols and interdisciplinary scientific competences, must be combined to solve identification and characterization issues in archaeometry. Indeed, not

only experts of different disciplines, including mineralogists and petrographers, historians, anthropologists, material scientists (etc.), but also the application of many different analytical techniques, such as spectroscopies, chemical analyses, imaging techniques, etc., are involved in archaeometric studies [17,18,21,22].

2. Cultural Heritage and Gemstones

The use of gem materials as ornaments, art expression, social state indicators, votive offerings, religious symbols, etc., is as ancient as humanity is old [23–29]. In fact, the properties able to fascinate humankind, characteristic of the gemstones, are beauty, rarity, and durability. These three qualities also correspond to the proprieties a material must have to be defined as a gemstone, even today. Indeed, the term gemstone includes many different types of materials: inorganic (i.e., diamond, corundum, jadeite, etc.), organic (i.e., amber, etc.), biogenic (i.e., pearl, coral, etc.), transparent to opaque, single crystal or polycrystal gemstones, etc., as long as they show beauty, rarity, and durability characteristics [30]. Therefore, unique objects have been given to us from ancient times, setting marvellous stones.

For these reasons, several studies have been conducted in collaboration with the world's most well-known-international gemological institutes. Among all of these studies, we can cite the example of the characterization study of the Talisman of Charlemagne, for which Panczer and co-authors (2019) [31] identified all the gemstones set (nine lateral stones, eight pearls, and one central stone for each talisman side, plus nine lateral stones and eight pearls set on the talisman's border) and hypothesized a Sri Lankan (Ceylon historical mines) origin for the huge sapphire set on the backside of the talisman, due to scientific gemological analyses. Another one is the study of the Iron Crown, kept at the altar of the Teodolinda Chapel in the Cathedral of Monza (Italy). The crown which has uncertain dating [32] sets a total of 22 gemstones [33], identified by Riccardi [33] as corundum (7), garnet (7), quartz (4), and artificial glasses (4). In addition, in this second case, a Sri Lankan origin has been hypothesized by the authors for the corundum gemstones. Regarding the multidisciplinary protocols, the characterization study of the Chiaravalle Cross can be considered as an example. Indeed, this cross is a medieval masterpiece belonging to the Duomo of Milan Museum collection (Italy), where a total of 985 gemstones are set, including four Trapiche Sapphires representing the first Trapiches found in history, and has been studied and used to develop a specific multidisciplinary protocol, involving experts of many different disciplines [34].

The collaboration with the gemological institutes for cultural heritage studies is focused on the characterization of sample-setting gemstones, but is not only limited to it. In fact, although it might seem unusual that a gemological institute can help the world of archaeology/cultural heritage sciences, for more than one reason, those disciplines can be successfully combined. Indeed, one of the main tasks performed by a gemological institute is to identify gem materials. To do that in a more modern acceptation of "scientific gemology", advanced analytical techniques (i.e., spectroscopic or chemical analyses) are required, with a specification of analyzing the sample without any preparation. Similar to that concerning modern gemstone studies, the artworks, archaeological samples, and *objets d'art* show the same analytical problems because they cannot be analyzed by destructive techniques. Thus, similar problems require similar analytical strategies. This is the reason why the equipment available at the internationally recognized gemological institutes is also suitable for archaeometric analyses. In fact, all of the high-tech equipment available in such institutes are equipped with accessories that allow the analysis of *tal-quale* samples [35–38].

In addition, several other considerations have to be taken into account: the gemological institutes are experts in gem materials' treatments, simulants, and imitation identification which cover, by definition, a huge class of materials (i.e., inorganic, organic, crystals, amorphous, biogenic, etc.). It means that it is possible to profit from this expertise; not only for gemstone identification and characterization, but also to recognize eventual counterfeiting. Indeed, some authors report several issues correlated with the authenticity of objects

even within collections of museums [20,21,34,39–42]. Since some samples may have no documented or incomplete provenance, a gap in information and authenticity doubt is possible [43–45]. Drayman-Weisser (2007) [46] reported an interesting case of a Renaissance enameled pendant jewel belonging to the collection of the Walters Art Museum: a deep archaeometry investigation revealed that the *Personification of Fortitude* pendant represents an embellishment of the former Renaissance jewellery because none of its parts are original.

Finally, due to the trade demand, in the past two decades, several gemological institutes have worked hard to increase the knowledge and analytical protocols for geographic origin determination, including the creation of huge collections of reference stones [47–50].

For all these reasons, gemological competencies can be included in the multidisciplinary approaches to cultural heritage and archaeological studies.

3. Analytical Techniques Available

In this paragraph, a brief overview covering the standard gemological tests to the spectroscopic and chemical analyses, useful also for archaeometric studies, has been reported.

3.1. Standard Gemological Tools and Analyses

In a gemological laboratory, a sample is firstly described based on its morphological characteristics, such as weight, shape and cutting style, dimensions, transparency properties, luster, optical phenomenon (if present), and color. Particularly for the color description, standard daylight is required, and the observation must be conducted in neutral conditions. Following international rules [51–53], the color is expressed by tone, hue, and saturation in the tridimensional colors system [54].

Regarding the other standard gemological tests, applicable also to the cultural heritage and archaeological samples, a brief discussion related to the main one is reported below.

The refractometer is probably the most important standard gem-testing instrument. It is used to establish a gem's refractive index (RI) and birefringence, determine whether the gem is singly refractive (SR) or doubly refractive (DR), and establish what its optic character and optic sign are. Using the refractometer along with the correct technique, the quick identification of a wide range of polished gem materials is possible. The lowest limit for an RI reading is about 1.35, while the highest is determined by the RI of the contact liquid used to perform the analyses (it is usually about 1.80) [55–57].

The polariscope can help to determine if a gem is SR, DR, or an aggregate (AGG), and it can also test for optic character or even detect pleochroism [58]. A gem must be transparent (TP) to translucent (TL) for testing with the polariscope; opaque (O) and semi-translucent (STL) stones could give unreliable information.

The dichroscope is a compact, portable instrument and is equally useful on rough and fashioned gems. It is designed to detect two of the different colors that pleochroic gems show in most viewing directions, and thus helps to confirm whether a gemstone is SR or DR [55,59].

Generally, the gemological handheld spectroscope can provide crucial information to help detect a treatment or identify a synthetic. Indeed, this useful portable small instrument can show the absorption in the visible light spectrum (400–700 nm), correlated with the colors' causes [60]. In addition, it does not require a polished surface, so it can be applied on rough or mounted gem material and also loose gems.

By the hydrostatic scale, the specific gravity (SG) of a sample can be calculated. To do that, the scale requires a particular accessory consisting of a holder for a beaker of water that sits above, but it does not touch the scale's weighing platform. A wire stand sits directly on the weighing platform and allows an object to be suspended in the beaker for weighing. The SG corresponds to the ratio between the object's weight in air and the weight in water minus the weight in air [55,61].

Regarding the stone's hardness, it is not a classical gemological test, due to its micro destructive nature, but it can occasionally be applied, for example, in rough characterization. To perform the Mohs scale test, sets of so-called hardness pencils are commercially available

and, courtesy of optical microscopy observation support, it is possible to determine the sample's hardness value [62].

3.2. Optical Microscopy (OM) and Imaging Systems

Regarding imaging and measurements, optical microscopes can be considered a useful tool for cultural heritage samples and gemstones, as well. A gemological microscope is a stereo binocular microscope with a good depth of field, generally with magnification varying between 10× and 80×. A microscope offers many lighting options. Different types of lighting work best for observing various gem features. The most used lighting in gemology is the darkfield, but transmitted, reflected, and diffused light can also be used [55,63].

Not only visible light can be considered, but also the fluorescence imaging systems can supply information by applying ultraviolet (UV) sources. Indeed, the Wood lamp test, by exposing the sample to the UV Short Wave (SW), 254 nm, and UV Long Wave (LW), 365 nm, can help separate certain natural gems from their synthetic counterparts, if a stone is assembled or several impregnation substances are present [56]. Moreover, in the 90s, the Diamond Trading Company (DTC) (DeBeers Group) developed the DiamondView™ instrument with the aim of separating the natural from the synthetic diamonds, on the basis of the growth patterns shown by the excitation of a shorter UV source (225 nm). Courtesy of a digital camera, pictures can be acquired in visible and UV modes and at different magnifications. The application of this instrument also for colored stones analyses demonstrated its availability to highlight many diagnostic characteristics of this type of material [64].

3.3. Spectroscopies

Three lines of spectroscopies can be considered, in a complementary way: micro-Raman (and Raman) spectroscopy, micro-Attenuated Total Reflection/Fourier Transform Infrared (micro-ATR/FTIR) or classical ATR and FTIR spectroscopy, and Ultraviolet-Visible-Near-IfraRed (UV-Vis/NIR) spectroscopy. While the first two lines represent very useful techniques for material identification, based on their characteristic vibrational modes, the last one is exceptionally suitable for obtaining detailed information about chromophores elements/groups and/or transitional metals, even if in traces.

Below is a brief description of those techniques and their applicability.

The "Raman" effect was discovered in 1928 by Indian physicist Sir. C. V. Raman, who observed a faint wavelength shift between a light source (monochromatic) and light returned after the interaction with a sample. In a typical Raman experiment, monochromatic radiation (the laser source) is used to excite the sample. The available laser sources belong to UV, visible, and Near-InfraRed (NIR) spectral regions. Thus, the Raman scattered light will also be in the visible region if visible excitation is used. No energy is lost for the elastically scattered Rayleigh light, while the Raman scattered photons lose some energy corresponding to the specific vibrational modes of the sample [65]. Among the many advantages of this technique, the main ones are: it is a non-destructive technique and does not require any sample preparation; the spectrum is characteristic for every mineral phase, similar to a "fingerprint" [66]; the technique proves to be very suitable for material identification, by the comparison with reference spectra [67]; and, finally, the spectroscopes can be coupled with an optical microscope, in order to perform the analysis in a confocal way [68,69].

The infrared spectrometer uses IR light as a source. These wavelengths can be absorbed, transmitted, or reflected by the analyzed sample. This instrument is particularly suitable for material identification in gemology [70], such as epoxy-resins, oils, plastic, and other substances used for colored gemstone treatments, especially the impregnations for clarity enhancements. They have distinct features in their infrared spectra and can be detected by the spectrometer. For gemstones, cultural heritage, and archaeological samples analyses, the sample preparation required by classical FTIR systems represents a significant

limitation. This limit can be overpassed due to the development of several accessories, such as the integration sphere, beam condenser, and ATR [64,71]. The latest evolution of this technique is represented by the micro-FTIR/ATR system: an integrated module equipped with an optical microscope, able to combine the classic FTIR analyses in spatially performing to the sample's morphology. The main advantages are the increase of spatial resolution and the analysis performed without sample preparation, especially in the case of micro-ATR acquisition mode [71–73].

The UV-Vis/NIR spectrophotometer uses a narrow beam of light in the electromagnetic spectrum between the UV and the NIR, across the visible wavelengths, as a source. A system of lengths focuses the light beam on the gemstone/sample. Those light wavelengths not absorbed by the sample are transmitted to the detector. UV-Vis/NIR spectroscopy aims to observe and characterize several elements present in the samples (i.e., the chromophore groups, transitions elements, etc.) on the basis of their characteristic absorption bands. Researchers typically use this information to determine the material's cause of color [74]. Although this technique traditionally requires sample preparation, courtesy of the latest generation of accessories (i.e., integration sphere), the instruments allow the analysis of transparent as well as opaque samples without preparation [75]. Moreover, by applying an optical fiber system to the spectroscope, it is possible to obtain an adaptable and portable instrument [76]. In gemology, this technique is usually associated with the classical manual spectroscope, which shows the gemstone absorption bands limited to the visible range of the light spectrum.

3.4. Complementary Chemical Analyses

The chemical information is a fundamental test for gemstones, cultural heritage, and archaeological sample identification and characterization. In fact, parallel to the main elements constituting the phases, the particular assemblage of trace elements (i.e., those present and their concentrations) provides a distinctive chemical signature for many gem materials [21,77]; therefore, different techniques can be considered. The first is Energy Dispersive X-ray Fluorescence (ED-XRF, or only XRF), due to its more straightforward applicability. At the same time, in case the sample characterization requires bypassing the limits of this technique, the chemistry information can be increased based on the Scanning Electron Microscopy with Energy Dispersive Spectroscopy (SEM-EDS) and/or Laser Ablation Inductively Coupled Plasma Mass Spectrometry (LA-ICP-MS) application.

ED-XRF is a technique whereby a sample is targeted by a high-energy X-ray beam, causing its chemical elements to fluoresce with a spectrum of lower-energy X-rays, with each peak being characteristic of a chemical element. The fluorescent X-ray peak intensities indicate the relative concentrations of the chemical elements. The range of detectable elements goes formally from sodium (Na) to uranium (U), with different detection limits, typically higher for the lighter elements and lower for the heavier ones; nevertheless, the concentration range goes from ppm levels to 100% [78]. The main advantages of this technique are that it does not require any sample preparation and the relative speed of the analysis. Because of all these advantages, ED-XRF has become one of the high-tech routine analyses for gemstone characterization [55]. More recently, Portable XRF (PXRF) instruments have been developed, with many successful applications in archaeometric studies among others. Although the PXRF actually cannot substitute *in toto* the lab-based counterpart, the possibility of on-site chemical analysis supplies extremely useful information in many archaeological and museum applications [79], even if the detection limits are lower.

On the other hand, by SEM-EDS, the chemical information can be combined with the sample morphology at very high magnification; moreover, by EDS, several lighter elements (nominally from boron) can be detected, but this technique generally requires sample preparation. The one exception to this is the Variable Pressure (VP-SEM) or Environmental pressure (E-SEM) application. In fact, by the aqueous vapor-controlled injection in the camera, the metal coating to increase the conductivity of the sample requested by the classic

SEM-EDS technique can be bypassed. Nevertheless, quantitative chemical data cannot be collected in VP or E-SEM conditions, but only semi-quantitative information can be acquired [80].

LA-ICP-MS is a micro-destructive technique able to detect almost all the chemical elements with detection limits in the range of parts per million (ppm) to even parts per billion (ppb) levels [64,81,82]. A typical gemological instrument set-up requires a single quadrupole ICP-MS. However, several laboratories are equipped with the last generation of a triple-quadrupole instrument, coupled with a 213 nm or 193 nm laser ablation unit. With the high-performance level of the techniques, as well as a considerable work of protocols development performed by the different research teams, the diameter of the ablation holes on the cut and polished stones have been reduced from about 50 µm to 30 µm. This fact must be considered a crucial goal for the standard application of the technique on gemstones because usually at least three to five spots are analyzed for each stone, focusing the laser ablation on the girdle.

It must be noted that all the chemical techniques previously described require suitable sets of standard samples, not always available and sometimes to be created ad hoc.

The advantages, limits, and complementarity of those techniques will be discussed in detail in the present review, on the basis of their application to Green Stones.

4. The Example of the Green Stones

Identifying and characterizing "Green Stones" is a complex work due to their considerable heterogeneity. Indeed, "Green Stones" is an "umbrella term" covering different types of materials, including but not limited to jade. Due to their characteristic attractive green colors and high toughness, these materials have been very appreciated by humanity for ornamental purposes since antiquity to modernity.

Considering cultural heritage samples and modern objects made of Green Stones, another common characteristic must be underlined: this group of gems are not single crystals (as per many other gemstone qualities) but are massive varieties, constituting aggregates of minerals. Moreover, these aggregates are rarely mono-mineral but usually show mineralogical associations. Thus, from the petrographic point of view, we have to identify rocks.

Compared to a single crystal gemstone, inevitably, this heterogeneity of the materials affects the identification procedure, at least from three different points of view: the analytical techniques useful and applicable; the identification and quantification of the minerals, in terms of relative phases distribution; and the nomenclature. In addition, the origin question is another discussion point, extremely useful for archaeological studies, but it represents a delicate analytical issue due to the limits of the characterization of the sources [83].

4.1. The Nomenclature of the Green Stones

One of the main issues related to Green Stones terminology is that the terms used to identify the materials belong to different disciplines, mixed together: gemology, cultural heritage, archaeology, mineralogy, and petrography. A brief discussion about the principal ones is reported below.

"Jade" is a common trade term, and in the gemology field, it is applicable to identify objects made by only two gemological species: jadeite and nephrite [30,84,85]. This clarification is significant because, by this acceptation, it is possible to individuate the objects with the highest quality from several points of view within a huge group of materials. Particularly, nephrite gemological species identifies a rock originated from a solid solution of the amphibole group minerals actinolite and tremolite, composed of an interlocking mass of granular and acicular crystals without a preferred orientation. On the other hand, jadeite is a pyroxene mineral phase, and in gem-quality jadeite, columnar and/or granular crystals are aggregated. Moreover, in gem-quality jade, jadeite and nephrite are not the only minerals present: associations are common. For example, in jadeite, the presence of augite, diopside, aegirine, omphacite, and kosmochlor are expected, but to be defined as

jadeite-jade, the dominant phase must remain the jadeite with the other phases in traces. In fact, only a high grade of purity of mineral aggregation is able to guarantee the hardness, toughness, and durability characteristics for which jade has become famous all over the world.

The modern term jade reflects in its acceptation the antique etymology of the material. Indeed, these terms come from the old Spanish etymology: jade derives from "piedra de la ijada", a Spanish expression meaning "stone of the loins", from Latin "*ilia*" ("hip") [86,87]; and nephrite has its origin in the Spanish "piedra de los riñones" or "stone of the kidneys" [88]. It is interesting to note that the conquerors of the New World indicated by this second term the jade worn used by the indigenous people who believed in its healing properties [86]. Traces of the same therapeutical application are reported by Salviati [89] regarding the Medici family of Florence during the Renaissance. Although there are not previous etymological clues on the western side of the world, and though the Romans did not appreciate the jades from what we know because they considered them to be unlucky, it is a fact that objects man-made in "jade" materials, such as ceremonial insignia and weapons, objects symbolizing the social status of their owners, and ritual and funerary artifacts, have been found in a different part of the world since the Neolithic Age [85,90–95], attesting the high level of consideration for this material in ancient civilizations.

On the other side of the world, in China, where a tradition of Green Stones use is well-documented since Neolithic times, the term "Yù"—literally "the most beautiful stone"—was used to describe not only jade but also other Green Stones, such as chalcedony and marble, that were carved into tools and ceremonial objects [87]. In the Chinese understanding, the corresponding term of jade was historically split into other two terms: Ying Yù (hard jade), also known as "Fei Cui", and Ruan Yù (soft jade), corresponding to the pyroxene varieties and other Green Stones, respectively.

While the Laboratory Manual Harmonisation Committee (LMHC) and the World Jewellery Confederation (CIBJO) are very straight for jade definition [30,84], the same clarity is not always applied. Thus, when the term jade is used as synonymous with the Chinese "Fei Cui", or as a direct translation of it, several misunderstandings in the material identification can occur. Indeed, different eastern countries use the term Fei Cui to identify different materials. For example, in Japanese, the term Fei Cui is a synonym for jadeite-jade. However, in the Chinese market, omphacite and kosmochlor "rich members" of the pyroxene group are often included in the term Fei Cui or, as per the Hong Kong trades, even "pure" omphacite and/or kosmochlor phases can be included under the Fei Cui umbrella term [96,97].

This overlapping of historical terminology with modern acceptation can generate misunderstandings that must be considered when cultural heritage samples and *objets d'art* are identified.

Another term used in the Green Stones panorama is Maw-Sit-Sit; it identifies a gem species corresponding to a green rock constituted by a variable mineralogical association and described for the first time by E. Gubelin in 1965 [98]. In fact, Maw-Sit-Sit is the name of the Himalayan village close to Tawmaw (Myanmar), where this gem material is usually extracted. It must be noted that different authors reported different mineralogical associations characterizing the Maw-Sit-Sit. Gubelin [99] described the Maw-Sit-Sit as a rock mainly composed of albite and Cr-jadeite; Manson [100] identified natrolite and kosmochlor as the main constituents; Hanni and Meyer [101] found chromite, kosmochlor, and Cr-amphibole as the main minerals, and finally, Colombo [102] demonstrated a composition of albite and kosmochlore as main phases, with chromite, eckermannite, and natrolite as associated phases for Maw-Sit-Sit from Myanmar. This heterogeneity in the mineral associations reflects the variability of the parent rocks, derived from the complex metamorphic system of the Myanmar area.

Considering the Green Stones, another big family eventually included is the crypto and micro-crystalline quartz species, such as chalcedony (chromium or chrysoprase varieties), jasper, and quartzite rocks. Indeed, this species can show several types of colors, including

green. Although the common basic unit consists of quartz crystals, the relatively significant heterogeneity of this class of gem materials must be noted. In fact, considering the jasper and chalcedony species, they are typically in hydrothermal (fluids precipitation product) and sedimentary environments [103,104], while quartzite is a typical metamorphic product. As per the variety name, in the Cr-chalcedony variety, the green color is correlated with the chromium element as chromophore [105]; on the other hand, the characteristic "apple green" variety of the chalcedony species is the chrysoprase [106].

In addition to these, several other mineral phases are ascribable to Green Stones. Pyroxenes such as kosmochlor, diopside, and omphacite have been already listed as associated minerals in jadeite or Maw-Sit-Sit, but they can also be identified as a single phase or dominant phase, characterizing the material analyzed. Moreover, belonging to Green Stones, other mineral phases can be listed, i.e., hydrogrossular and grossular, vesuvianite (californite, variety), or pumpellyite.

Finally, a significant phase belonging to Green Stones is serpentine. By this term, three different polymorphs (minerals having the same chemical composition but different crystal structures) are identified: lizardite, antigorite, and chrysotile. While the first two are typically massive, the last one is of the fibrous variety. Chrysotile is unwillingly quite famous because it is listed as one of the six fibrous minerals identified by the law as "asbestos", and is hazardous to human health [107].

By this short overview of the main materials classified as "Green Stones" and their definition (summarized in Table 1), underlying their heterogeneity, the importance of the proper jade and related-to-jade materials identification for archaeological, cultural heritage studies, and antiquity trades becomes understandable [108]. A proper material identification represents the base of a good archaeometric work and, consequently, the base of archaeological or cultural heritage considerations. For example, the discussion about the origin or the technology applied for artifact creation is strictly related to the materials' properties and characteristics. Thus, the archaeometric analysis of Green Stones helps archaeologists to find answers.

Table 1. The nomenclature of "Green Stones".

Term	Definition
Jade	**Trade name** applicable to gem materials made only by jadeite or nephrite.
Jadeite	**Gemstone Species–Mineralogical phase**; piroxene mineral, columnar and/or granular crystals are aggregated.
Nephrite	**Gemstone Species**; a rock originated from a solid solution of the amphibole group minerals actinolite and tremolite, composed of an interlocking mass of granular and acicular crystals without a preferred orientation.
Fei Cui	**Trade and historical name**; traditionally translated as "hard jade".
Maw-Sit-Sit	**Gemstone Species**; green rock constituted by a variable mineralogical association (i.e., albite, kosmochlor, chromite, eckermannite, natrolite, etc.) found in the Himalayan area.
Chrysoprase	**Gemstone variety**; "apple green" variety of chalcedony species—cryptocrystalline quartz.
Cr-chalcedony	**Gemstone variety**; green variety of chalcedony species—cryptocrystalline quartz.
Green Jasper	**Gemstone variety**; green variety of jasper species—microcrystalline quartz.
Green Quartzite	**Rock** (metamorphic), constituting mainly by quartz mineral associated with green phases (i.e., diopside, etc.).
Serpentine	**Gemstone Species—Mineral polymorphic phase**; three different polymorphs (minerals having the same chemical composition but different crystal structures) are identified: lizardite, antigorite, and chrysotile.
Californite	**Gemstone variety**; green massive variety of vesuvianite (idrocrase) species.
Diopside Omphacite Kosmochlor Pumpellyite	**Gemstone Species–Mineralogical phases**; piroxene minerals.
Hydrogrossular Grossular	**Gemstone Species–Mineralogical phases**; belonging to garnet group.

4.2. Classical Gemological and Mineralogical Properties

Beside the terminology discussed in Section 4.1, the main Green Stones materials' gemological and mineralogical characteristics have been reported in Tables 2 and 3, re-

spectively. In both tables, the extreme heterogeneity of these materials is underlined. On the other hand, the presence of similarities cannot be neglected; in addition to the color, consisting of practically all the green hues and tones, the optical character, reported as AGG (Table 2) for all of the species, reflects the massive variety of the materials under discussion. Another common characteristic is hardness, which is reported based on the Mohs scale and ranges from 5 to $7\frac{1}{2}$. The one exception is the hardness of serpentine, which is lower, but it must be noted that the range reported corresponds to the pure phase, while the association with other minerals, widespread in serpentine objects, can increase it and allows the curving cut.

Table 2. Classical gemological and mineralogical properties of Green Stones [56,62,109–112]. Here, the characteristics of massive varieties have been preferred compared to the single-crystal counterparts, due to the highest diffusion of the first ones in cultural heritage studies, and, according to the topic, only the green varieties (and not other colors) have been considered. The reported data correspond to the natural untreated varieties; eventual synthetic, treated, or imitation counterparts have not been considered. RI = Refractive Index; SG = Specific Gravity; AGG = Aggregate Reaction; DR = Doubly Refractive; STP = Semitransparent; TL = Translucent; STL = Semitranslucent; O = Opaque; LW = Long Wave (365 nm); SW = Short Wave (254 nm).

Species and Variety	General Description	RI	SG	Optical Character	Transparency	Fluorescence	Mohs Grade
Jadeite	Light to dark green, often with uneven coloration, mottling, or root-like markings. Vitreous to greasy polish luster with a dimpled polished surface, granular to splintery fracture with dull fracture luster.	1.666 to 1.680 (+/−0.008) 1.66 spot reading common	3.34 (+0.06/−0.09)	AGG	STP to O	LW: None to Faint White SW: None	6
Nephrite	Light to dark green, possibly with lighter or darker mottling. Vitreous to greasy polish luster, splintery to granular fracture with dull fracture luster.	1.606 to 1.632 1.61 spot reading common	2.95 (+0.15/−0.05)	AGG	TL to O	LW: None SW: None	6–6$\frac{1}{2}$
Serpentine	Usually yellowish green, green, or greenish yellow. Waxy to greasy polish luster, granular to uneven fracture, with dull to waxy fracture luster.	1.560 to 1.570 (+0.004/−0.070) 1.56 spot reading common	2.57 (+0.23/−0.13)	AGG	STL to O	LW: None to Med chalky (B, W, and G) SW: None	2$\frac{1}{2}$–3$\frac{1}{2}$
Maw-Sit-Sit	Opaque saturated green rock with characteristic dark green to black veining or mottling. Waxy to vitreous polish luster, granular fracture with dull fracture luster.	Spot readings around 1.53 to 1.74 (Multiple readings result from combination of different minerals)	2.77 (+0.38/−0.31)	AGG	O	LW: None SW: None	6
Hydrogrossular (Garnet Group)	Green to bluish green. Might show black inclusions. Vitreous polish luster, uneven, granular, or splintery fracture with greasy to vitreous fracture luster.	1.720 (+0.010/−0.050) 1.72 spot reading common	3.47 (+0.08/−0.32)	AGG	TL to O	LW: None SW: None	6–7$\frac{1}{2}$
Vesuvianite (Idocrase), Californite variety	Yellowish green, green, brownish green. Vitreous to greasy polish luster, granular fracture with vitreous to dull fracture luster.	1.713 to 1.718 (+0.003/−0.013) 1.70 or 1.71 spot reading common	3.40 (+0.10/−0.15)	AGG	TL to O	LW: None SW: None	6–7
Diopside	Bluish green to yellowish green. Chrome diopside is intense green. Vitreous polish luster, conchoidal to uneven fracture with vitreous to resinous fracture luster. Massive and may show splintery to granular fracture.	1.675 to 1.701 (+0.029/−0.010)	3.29 (+0.11/−0.07)	DR (single crystal) AGG (massive)	TL to O (massive)	LW: None to Med Green SW: None	5$\frac{1}{2}$–6$\frac{1}{2}$
Omphacite	Green to dark green. Brittle tenancy with fracture uneven, conchoidal and luster vitreous, silky.	1.662–1.723 1.68 or 1.71 spot reading common	3.16 to 3.43 [1]	AGG	O	LW: None to Med chalky (B, W, and G) SW: None	5–6
Pumpellyite Group	Blue–green, dark green to white fibrous to lamellar masses with glassy luster.	1.674 to 1.764	3.20 to 3.30 [1]	DR (single crystal) AGG (massive)	TL to O	LW: None SW: None	5–6
Chalcedony (chrome or chrysoprase variety)	Green to slightly bluish green. Greasy to vitreous polish luster, conchoidal fracture with dull to waxy fracture luster.	1.535 to 1.539 (1.53 to 1.54 spot reading)	2.60 (+0.10/−0.05)	AGG	STP to STL	LW: None SW: None	6$\frac{1}{2}$–7

[1] SG for omphacite and pumpellyite group has been reported by its range according to the references.

Table 3. Main mineralogical characteristics of Green Stones species here discussed [96,113,114]. For the series, the chemical formula of the end member/pure phase has been reported.

Mineral Phase	Chemical Formula	Group/Family	Crystal System
Jadeite	$NaAl[Si_2O_6]$	Clinopyroxene	Monocline
Actinolite [1] Tremolite [1]	$Ca_2(Mg,Fe)_5[Si_2O_6](OH)_2$ $Ca_2Mg_5[Si_2O_6](OH)_2$	Amphibole	Monocline
Lizardite [2] Antigorite [2] Chrysotile [2]	$Mg_3[Si_2O_5](OH)_4$	Trioctahedral Phyllosilicate	Trigonal Monocline Orthorhombic
Albite [3]	$Na[AlSi_3O_8]$	Tectosilicate, Plagioclase Feldspar	Triclinic
Kosmochlor [3]	$NaCr[Si_2O_6]$	Pyroxene	Monocline
Chromite [3]	$Fe^{2+}Cr_2O_4$	Oxides, Spinels	Cubic
Eckermannite [3]	$Na_3Mg_4Al[Si_8O_{22}](OH)_2$	Amphibole	Monocline
Natrolite [3]	$Na_{16}[Al_{16}Si_{24}O_{80}]\cdot 16H_2O$	Tectosilicate, Zeolite	Orthorhombic
Hydrogrossular	$Ca_3Al_2(Si_3O_{12})\cdot(H_2O)_{2\text{-}6}$	Nesosilicate, Garnet	Cubic
Vesuvianite	$(Ca,Na)_{19}(Al,Mg,Fe)_{13}(SiO_4)_{10}(Si_2O_7)_4(OH,F,O)_{10}$	Sorosilicate	Tetragonal
Diopside	$CaMgSi_2O_6$	Clinopyroxene	Monocline
Omphacite	$(Ca,Na)(Mg,Fe^{2+},Fe^{3+})[AlSi_3O_8]$	Clinopyroxene	Monocline
Pumpellyite	$Ca_2MgAl_2(Si_2O_7)(SiO_4)(OH)_2\cdot H_2O$	Sorosilicate	Monocline
Quartz [4]	SiO_2	Tectosilicate	Trigonal

[1] Main mineral phases (pure end members) constituting nephrite gemological species. [2] Serpentine polymorphs, particularly the chrysotile is the fibrous variety of the mineral. [3] Main mineral phases constituting Maw-Sit-Sit variety. [4] Main mineral phase constituting chalcedony species.

In Table 3, the main mineralogical properties of the phases possibly found in Green Stones are reported. It must be noted that not only silicate minerals but also oxide minerals have to be considered for Green Stones. Moreover, regarding the silicates, all the families are represented.

As discussed in depth in the nomenclature section, correctly identifying the green stone phase represents a crucial point for gemology practice and cultural heritage studies. Thus, considering the heterogeneity and complexity of the materials, for their identification, a mineralogical characterization provides extremely suitable support, as attested by many archaeometric applications. Moreover, by the characterization of the phase, several information can be obtained, which could help, for example, in discussions about origins, colors factors, and mechanical properties considerations.

Despite all of this variability, observing the data reported in Table 3, several similarities can also be highlighted. Indeed, considering the pyroxene members, jadeite, kosmochlor, omphacite, and diopside are all minerals showing chemical and crystallographic affinities. In some cases, they can be found as components of metamorphic rocks, except for diopside, which can also be found as a component in some magmatic rocks (i.e., alkali olivine basalts). It is interesting to note that pure jadeite is a colorless mineral: only when a small amount of chromium (Cr^{3+}) goes inside the crystal structure as a substituting element of aluminium (Al^{3+}), jadeite can show its vivid "Imperial Green" color (Figure 2a), so called in modern and ancient trades. However, green Cr-rich jadeite does not become a kosmochlor only as a consequence of the substitutions. Indeed, the crystallization of a phase despite another one is not only a matter of chemical availability but also of the pressure and temperature conditions involved in the process. Jadeite genesis is such an example: almost all the known paragenesis involves the albite-jadeite association. If the metamorphic grade increases, the jadeite component decreases, giving way to omphacite

crystallization. In this condition of regional metamorphism, gabbro rocks can show veins rich in jadeite-pumpellyite association (Figure 2b) [114].

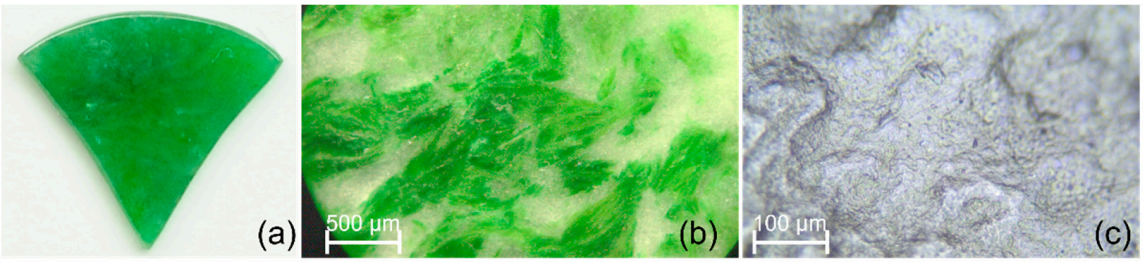

Figure 2. Jade aspect and texture details: (**a**) jadeite-jade, imperial green, Photo: M. Musa—Gemological Education and Certification Institute (GECI) reference stone collection: (**b**) jadeite-pumpellyite association (green veins) in albite white matrix (OM Image, 5× magnification, darkfield light), Photo: M. Musa—GECI reference stone collection; (**c**) nephrite-jade-polished cabochon surface, detail of its characteristic texture, where no iso-oriented acicular/columnar crystals are evident, but the grains are associated to elongated crystals, oriented in different directions (OM Image, 20× magnification, reflected light), Photo: M. Musa—Gulf Institute of Gemology (GIG).

This example can help to understand why the determination of geographic origin in Green Stones is so complex: not only different mines can produce similar materials, but also differences in terms of chemical and mineralogical distribution can be found within the same vein [90]. Moreover, from a multidisciplinary point of view, the knowledge of the geological process and the petrographic identification of the mining areas are necessary information for the geographic origin hypothesis [115].

The same consideration can be applied to amphiboles and serpentine, and both correlate with metamorphic processes. Serpentines, in particular, are typical products of the transformation of ultramafic rocks by a hydrothermal metamorphic system, while nephrite requires not only the conditions for actinolite-tremolite crystallization but also the condition for its characteristic texture (Figure 2c). Figure 2c, in particular, shows the sample detail where the interlocking mass of granular and acicular crystals without a preferred orientation are well visible. Regarding the nephrite genesis, Prokhor [116], describing for example the ultramafic complex of East Sayan, reported nephrite veins formation at the base of the ultramafic members of the ophiolitic nappes, as a consequence of the metamorphism and metasomatism resulting from frictional heating at the block-matrix contacts.

The hydrogrossular and grossular (Figure 3a) are garnets crystallized typically from the thermal metamorphic process applied to limestone. In the case of regional metamorphism, they can be associated with vesuviana and diopside and, finally, grossular can be associated with serpentine and found in rhodingite rock (Figure 3b,c).

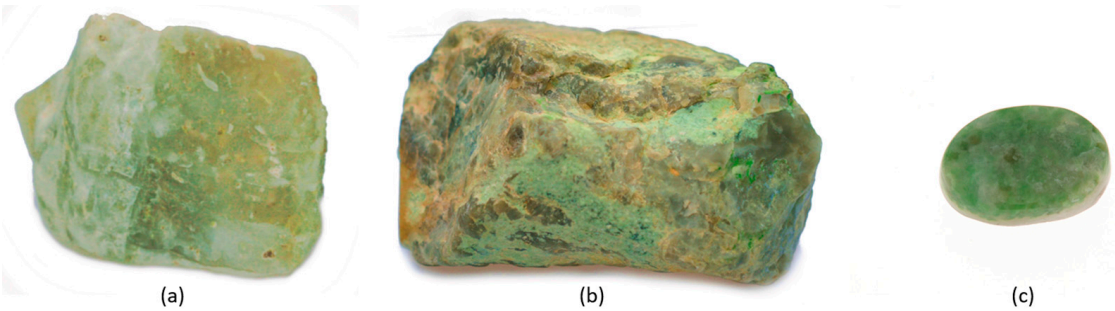

Figure 3. Mineralogical samples of (**a**) grossular/hydrogrossular and (**b**) grossular/hydrogrossular in rhodingite rock association; (**c**) rhodingite-polished tablet. Photos: M. Musa—GIG.

Finally, the chalcedony; the green variety can be mainly distinguished between chromium-chalcedony and chrysoprase (Figure 4). As per the variety name, in the first

case, the origin of the green color is correlated with chromium naturally present as a trace; on the other hand, the chrysoprase characteristic "apple green" color is due to a nickel-rich mineral associated with chalcedony, typically belonging to the garnierite mineral group [106]. The processes producing chalcedony are still under discussion; typically, quartz-rich fluid precipitation is hypothesized as a mandatory condition [117], whether the process is hydrothermal with crystallization in geodes or metamorphic.

Figure 4. (**a**) Chromium-chalcedony mineralogical sample (Photo: M. Musa—GIG) and (**b**) chrysoprase-polished cabochon (Photo: M. Musa—GECI reference stone collection).

So, starting from general observations, how can these materials be distinguished? First, a deep investigation of the sample visual characteristics is mandatory. As reported previously, applying the OM technique can significantly help the analyst to start several considerations about, for example, the homogeneity in terms of color, mineral distribution, or texture. For these purposes, extremely high magnification is not required: classical gemological darkfield stereo-microscopes are suitable, as well as the last generation of the digital portable optical microscopes (in case of an on-site analyses section).

Observing the data reported in Table 1, the importance of the RI and SG as key tests for the gemological material identification is evident, among others. Unfortunately, these tests are sometimes limited in application or with the reliability of their results. The RI requires three operative conditions: the homogeneity of the sample, a polished surface (better if flat), and the use of the refractometer contact liquid [57]. The first condition is difficult to apply to rocks, which are a mix of phases. This is the reason, as reported in Table 2, the RI technique is not applicable, for example, to Maw-Sit-Sit identification. The same issue can occur if we analyze a material made by jadeite mixed with other pyroxenes and/or albite. The second condition is more correlated with the surface characteristics of the samples. In fact, typical Green Stones objects are curved (i.e., double cabochons); therefore, a lecture on the flat polished surface is extremely rare. Thus, the spot reading is usually the only possibility for the RI test, but it is less accurate and obtained by a distance observation, without magnification. Moreover, additional limits correlated with the dimension of the objects, often largely sized, must be considered. Finally, the use of the contact liquid, even if perfectly safe for gemstones, can be absorbed by a porous object (i.e., serpentine) with the risk of consequent small stains, or it cannot be allowed by the conservation institutions policies, for example, in case of museum collections studies.

Regarding the SG test, it allows the gathering of important information regarding the density of the material, but again it is possible to encounter limitations of the technique. The most common method for the SG test in gemology corresponds to the hydrostatic weight. In this system, the water temperature, the homogeneity of the samples, and their dimensions and roughness can affect the precision of the measurement. In cultural heritage, especially the archaeological samples do not show well-polished surfaces, which can be very rough due to weathering and ageing. Such surface characteristics may easily entrap gas bubbles, altering the SG results.

Thus, considering the limited applicability of the RI and SG, an excellent analytical protocol for Green Stones samples' identification and characterization must include the application of high-tech techniques.

4.3. The Raman Investigation

Among other vibrational spectroscopic techniques, Raman spectroscopy is considered a powerful tool for identifying minerals and gemstones [66,118–120] (see Section 3.3). Because of its peculiarity, it represents a very suitable technique to solve the Green Stones identification problems [96,121].

Table 4 lists the main Raman features for quick identification of the Green Stones. In fact, considering only the main vibrations, the greater part of the phases constituting Green Stones can be easily distinguished.

Table 4. Raman main features characterizing Green Stones. The main bands of pure actinolite, tremolite phases, together with those of nephrite, and antigorite, lizardite, chrysotile phases, together with those of serpentine, have been reported as references for completeness.

Mineral Phase/Variety	Main Vibrations–Raman Shift (cm^{-1})				References
Jadeite	1039, 990	700			[96,120–123]
Nephrite	1060, 1032	674			[90,120,122]
(Actinolite)	1062, 1027	669			[90,124]
(Tremolite)	1062, 1031	676			[90,121]
Serpentine	1044	683, 635		378	[122]
(Antigorite)	1044	683, 635		375	[122,125]
(Lizardite)	1096 b	690		388	[125]
(Chrysotile)	1105	692		389	[125]
Albite[1]			510, 482		[120,122,123]
Kosmochlor [1]	950	683	(551−) 556, 522, 413 (−418)	340	[96,126,127]
Chromite [1]		690 b	560 b		[126,128]
Eckermannite [1]	1025, 992	690			[129]
Natrolite [1]			535, 443		[130]
Hydrogrossular	871			361	[131]
Vesuvianite	930, 862	643			[132]
Diopside	1010	666			[120,133]
Omphacite	1024	685			[92,122,123,134]
Pumpellyite	990, 920	697			[135]
Chalcedony			503, 465		[34,136,137]

[1] Main phases constituting Maw-Sit-Sit variety. b = Broad band.

The problem in the phase identification may occur only when the phases are characterised by the main vibrational modes within 2 cm^{-1} Raman shift: jadeite-pumpellyite (discussed later in this section), nephrite vs. its pure end members, and the serpentine polymorphs. In fact, ±2 cm^{-1} is the tolerance commonly accepted for Raman spectrum interpretation, especially when the analysis is carried out on a natural phase [120,121]. Regarding the nephrite, although actinolite is well recognisable, tremolite pure end member can hardly be detected. To overcome this issue, a deep morphological observation is mandatory. Indeed, as already described (see Section 4.1 and Figure 2c), nephrite must show its characteristic texture, while column-like and/or needle-like *habitus*, with isoriented crystals, are typical of actinolite and tremolite pure terms.

Regarding serpentines for gemstone species identification, both of the massive polymorphs, antigorite and lizardite, are accepted and both can be easily distinguished on the basis of their Raman features; nevertheless, the references report spectra more consistent with the first one [122]. On the other hand, chrysotile polymorph shows the main Raman bands strictly near to the lizardite ones. In this case, similar to the nephrite, morphological observation and OM analysis are very helpful because, as already reported, crysotile is the fibrous polymorph of the serpentine species.

Similar to Table 4, the same can be observed by the reference spectra reported in Figure 5, where all six spectra reported show relatively strong, sharp, and well-defined bands, as a consequence of the high crystallinity of the materials analyzed. Only the

omphacite phase shows Raman bands with characteristic Full Width at Half Maximum (FWHM) of the band amplitude higher than other phases (Figure 5), as diopside or jadeite. Generally speaking, by Raman spectroscopy, the higher the crystalline grade of the sample, the sharper are the scattered bands [65,119]. Nevertheless, to obtain reliable Raman spectra on Green Stones, the analyst has to pay particular attention to the choice of laser source. While for inosilicates, and silicates generally, a visible red source (i.e., 632.8 nm) could be one of the best selections, due to the high affinity of the wavelength with the silicon tetrahedra vibration [120], when the phase is Cr-rich, a strong fluorescence issue can be generated. On the basis of this consideration, the availability of a second source, for example, a visible green (514.5/532 nm) or NIR (785 nm) laser, could be a good option to solve the issue and complete the characterization. The fluorescence issue is one of the main limits of the technique [65]. This problem might be solved changing the source but multi-laser systems are not always available. Finally, surface sample treatments (i.e., waxing, varnishing, etc.) can generate Raman fluorescences.

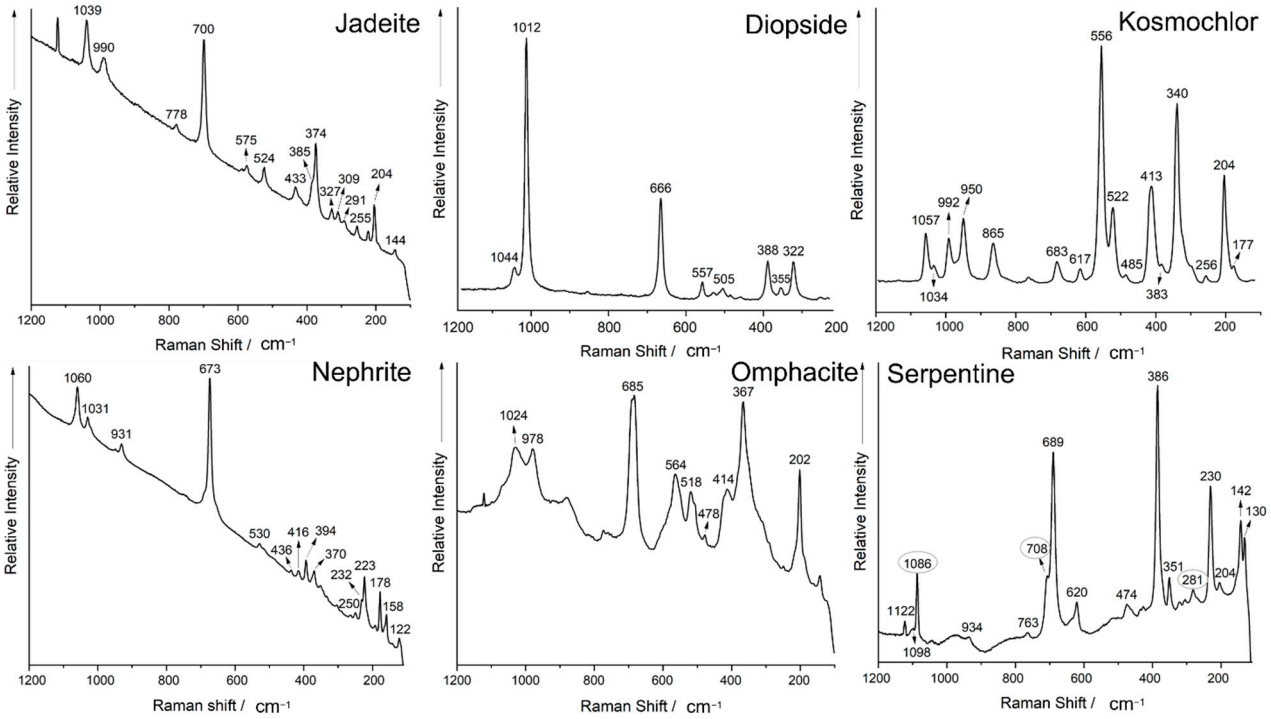

Figure 5. Reference Raman spectra of several Green Stones samples. Kosmochlor spectrum is re-plotted from the RRUFF reference N. R120015 [127]; the other spectra have been acquired by In-Via Confocal micro-Raman Spectroscope, Renishaw, 514.5/632.8 nm sources and elaborated using Origin 2020 software by the author on GECI Reference stones collection. Circled bands in the serpentine spectrum are consistent with calcite phase associated with serpentine.

Moreover, as previously mentioned, a potential difficulty could emerge in jadeite-pumpellyite identification, considering prudential tolerance of about 2 cm^{-1} Raman shift for the spectrum interpretation, correlated with possible substitutions and/or crystal lattice defects, which are very common in natural phases [90]. In fact, these two phases diverge for only a 3 cm^{-1} Raman shift on the main vibrational bands. In Figure 6, the reference Raman spectra of the two phases are reported. Despite the Raman shifts of the main vibrational bands being extremely close (700 vs. 697 cm^{-1}, see also Table 4), many differences can be highlighted by observing the trends of the entire spectra. The pumpellyite phase shows not only a spectrum richer in band numbers, but many of those bands are broader with respect to the jadeite ones, suggesting the presence of convoluted components [138].

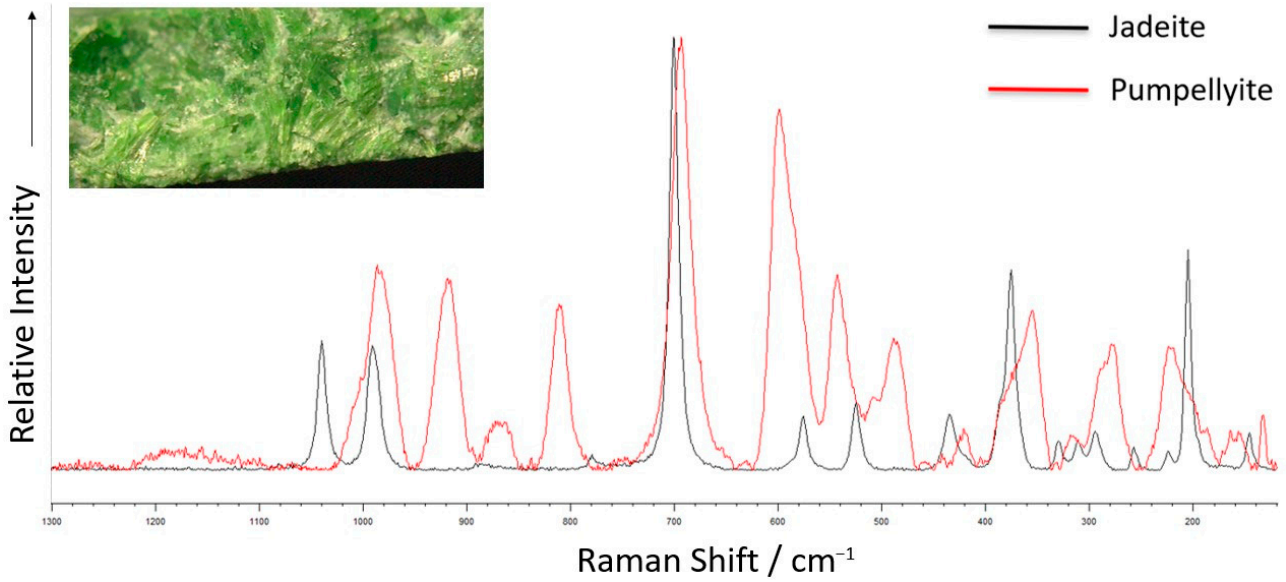

Figure 6. Overlap of jadeite (acquired by In-Via Confocal micro-Raman Spectroscope, Renishaw, 514.5 nm source by the author on GECI Reference stones collection); black line and pumpellyite (re-plotted from RRUFF N. R120172 [135]); red line, Raman spectra with baseline subtraction. The spectra have been elaborated by Wire 5.5 software. The top-left box shows the OM (5× magnification, darkfield) of a cabochon section of jadeite-pumpellyite association in albite matrix.

Moreover, for the diagnosis, the texture must again be considered; in the top-left box of Figure 6, the OM of a cabochon section of jadeite-pumpellyite association is reported, showing the presence of many green elongated crystals of pumpellyite and jadeite in a white matrix. This texture, not associable with jadeite-jade gem quality, is a consequence of the specific genesis of the sample and produces higher brittleness.

From an operative point of view, Raman spectroscopy has several advantages. The last generation of portable Raman spectrometers, in particular, exhibit very high versatility and due to optical fiber technology, several models can be easily coupled with a portable microscope. These set-ups allow the Raman characterization of Green Stones "on-site" by a micro-Raman system, which is extremely useful in the case of non-homogenous samples. In 2017, Gendron et al. [139] reported that a portable Raman spectrometer was employed in situ inside the Centro-INAH Veracruz reserve; during the short time available for the analyses, several El Manatì artifacts were analyzed with the main aim of verifying which artifacts were made of jade. By the application of this technique, the authors proved that a total of 11 artifacts, 10 axes, and 1 bead had been made by omphacite, instead of jadeite. Similarly, Zhao [140] reported the successful combination of a portable Raman system, applied with a portable XRF (PXRF) in a complementary way, for nephrite-jade artifacts characterization from the Cemetery of the Ying State (Henan Province, China). Courtesy of the application of the two techniques, the study revealed, among other results, the interesting presence of cinnabar pigment on the surface of the two jade artifacts, probably associated with religious rituals performed during the Western Zhou Period. On the other hand, a portable system is not able to substitute completely the benchtop counterpart, especially for the detectors resolution and mapping tools. Indeed, in recent decades, several micro-Raman mapping systems have been developed, allowing the complete spatially resolved interpretation of the data, particularly suitable for uneven samples. In other words, regarding Green Stones, the micro-Raman tool results in a suitable technique for testing phase distribution and homogeneity [90]. In Figure 7, an example of micro-Raman mapping on a green stone is reported. In particular, the sample analyzed by the line map tool comprised mainly quartz and diopside mineral phases. In fact, in this case, the map elaboration performed by a signal to baseline calculation shows the

relative spatial distribution of the two phases, on the basis of their main Raman bands (Figure 7, top-right): 666 cm^{-1} for diopside (range 662–672 cm^{-1}) and 465 cm^{-1} for quartz (range 461–471 cm^{-1}). Observing the plot of the blue and red lines, representing the spatial distribution of the two phases, a complementary trend in the relative distribution results is evident. This powerful tool also shows the correspondence between the single spectrum acquired (Figure 7, bottom), the spot position on the microscope sample's image (Figure 7, top-left), and the phases distribution by false-colors of the spots. Thus, the line map allowed not only to identify the phases but also to highlight their relative spatial distribution. The micro-Raman mapping systems not only allow the line maps, as already shown, but also the area maps, which is particularly useful when poly-phase samples have to be analyzed.

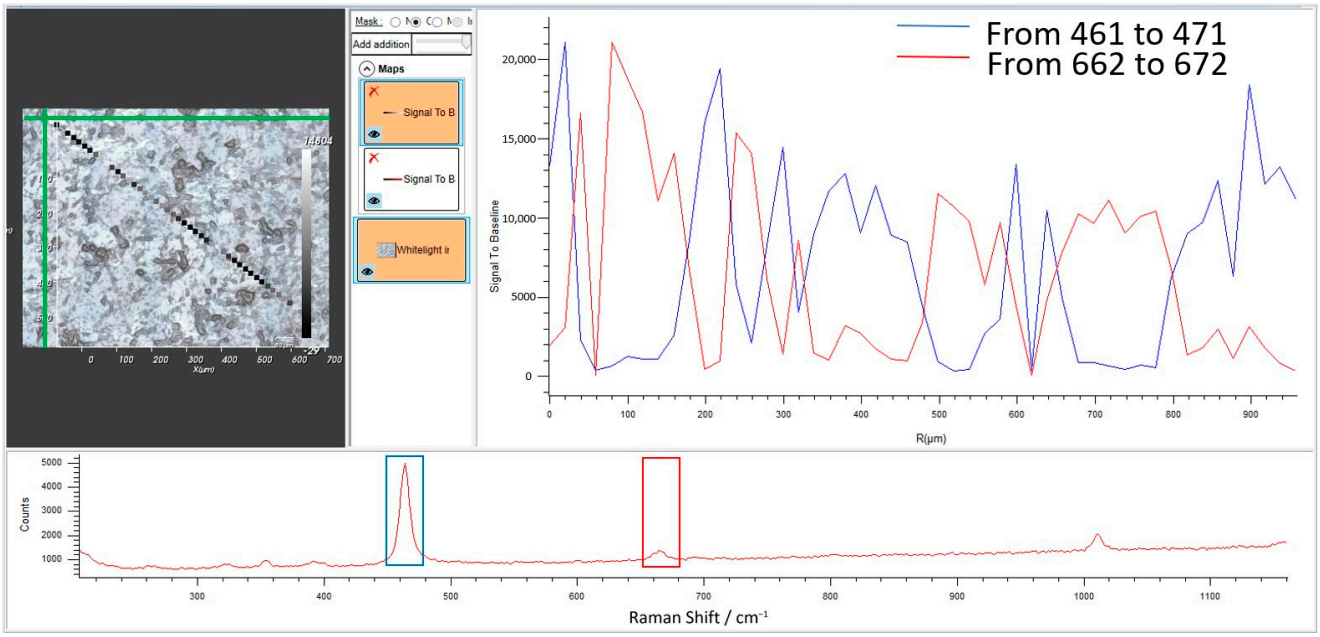

Figure 7. micro-Raman spectroscopy—line map tool applied for a green stone characterization, a diopside-quartzite rock, reported as an example of the technique's feasibility. (**Top-left**) MO image (20× magnification, reflected light) showing the mapping area on the sample surface and also the analyses spots; (**Top-right**) data results elaborated by signal to baseline method, considering the two ranges, corresponding to the main vibrational modes of diopside (red line) and quartz (blue line). Note the complementarity of the main bands' distribution related to the sample area where the signals have been detected, highlighted by the graph; (**bottom**) one of the spot analysis results, corresponding to the cross axes spot in the map image (green): blue and red squares correspond to the quartz and diopside main vibrational mode ranges, used for the elaboration. The map has been carried out using In-Via Confocal micro-Raman Spectroscope, Renishaw, 514.5 nm source, Wire 5.5 software. Data: M. Musa, GIG.

4.4. The Fourier Transform InfraRed Spectroscopy (FTIR) Investigation

The infrared spectrometer uses IR light as a source and is a technique belonging to vibrational spectroscopies. In cultural heritage and archaeometry applications, infrared spectra can help analysts and researchers to identify functional groups that characterize the materials or identify eventual gemstone treatments.

Regarding materials characterization, in Table 5, the main vibrational absorption features of the phases discussed in the present work have been reported.

Table 5. Infrared main vibrational absorption bands of Green Stones. The IR main bands of the pure actinolite and tremolite phases, along with nephrite, antigorite, lizardite, and chrysotile phases, along with serpentine, have been reported as references for completeness.

Mineral Phase/Variety	Main Vibrations–Wavenumbers (cm^{-1})				References
Jadeite	582	999	1090		[122,123,141–143]
Nephrite	686, 756	950, 995	1064, 1102	3660, 3676	[122,123,141,144]
(Actinolite)	668, 756	918, 942, 992	1066 b	3675	[144]
(Tremolite)	686, 758	920, 951, 990	1057	3673	[145]
Serpentine	471	990	1080	3671	[122,146,147]
(Antigorite)	436, 449 (−471), 617	962, (990–) 997	1084	3676	[146,147]
(Lizardite)	442, 621	976	1010, 1084	3687	[146]
(Chrysotile)	439, 609	949	1000, 1080	3649, 3685	[146]
Albite [1]		994	1040		[123,148]
Kosmochlor [1]		980	1114		[96]
Chromite [1]	520 b, 650 b				[149]
Hydrogrossular		840, 910		3660	[150]
Vesuvianite	482	900, 980	1011	3570	[151]
Diopside	456	860, 960	1065		[152]
Omphacite	448, 523	956	1060		[122,126,142]
Pumpellyite	440	947		3406, 3556	[153]
Chalcedony	450	780, 796	1067		[154]

[1] Several phases constituting Maw-Sit-Sit variety. b = Broad band.

Moreover, Figure 8 shows the absorption spectra of several mineral phases belonging to Green Stones. It is important to note that, different to what has been shown previously for Raman spectroscopy, several bands overlap between the phases, making more complex the identification, especially for minerals belonging to the same groups.

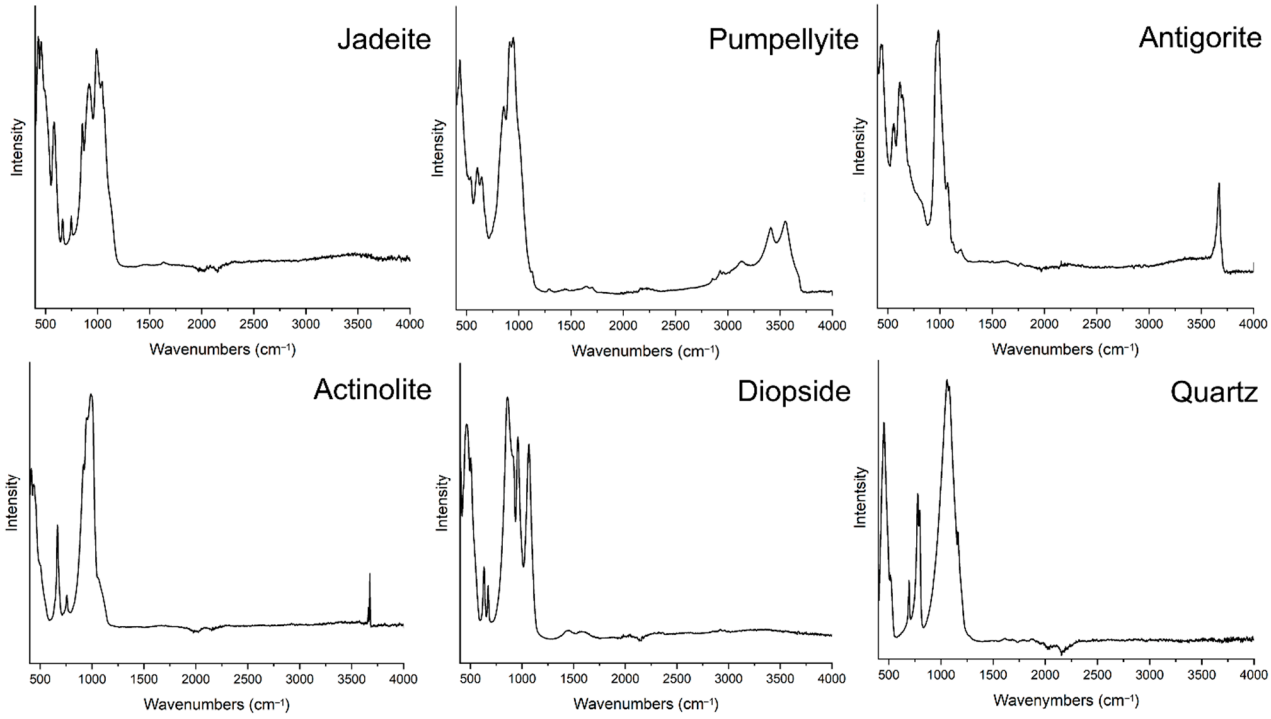

Figure 8. Reference IR absorption spectra of several Green Stones samples, re-plotted from RRUFF: Jadeite N. R050220-1 [143], Actinolite N. R040063-1 [144], Pumpellyite N. R070130-1 [153], Diopside N. R040009-1 [152], Antigorite N. R070228-1 [147], and Quartz N. R040031-1 [154]. Powder samples in KBr pellets, transmission mode. Spectra elaboration by Origin 2020 software.

This phenomenon is partially correlated with the characteristic broadening of the silicate absorption bands. Moreover, an operative consideration has to be made; the spectra reported in Figure 8 are re-plotted from RRUFF database files [143,144,147,152–154], collected from a powdered sample in transmission mode. In fact, very high-quality spectra

can be acquired by this method, though unfortunately this procedure shows some limits in cultural heritage or gemology studies. These limits can be partially bypassed: in recent decades, several accessories and/or modules have been developed to solve the problems correlated to the sample's preparations (i.e., integration spheres, Attenuated Total Reflectance—ATR, etc.). All of these accessories are mandatory in gemological and cultural heritage applications. As discussed above, using this set-up, the FTIR characterization can also be performed without any sample preparation on opaque materials, being extremely useful for poly-phases and uneven samples such as Green Stones. Unfortunately, although very useful, micro-FTIR is not a portable system.

On the other hand, the special affinities of the IR source with organic compounds make FTIR spectroscopy particular suitable to identify jade impregnation by organic substances treatments (Figure 9) [70,155,156]. As reported by Fritsch [156], it is interesting to note that in this modality, none of the fingerprint bands correlated with the most characteristic vibrational modes of the jadeite are detectable, due to detector saturation, while the presence of an extraneous compound such as resin, wax, or oil can be easily highlighted. Since antiquity, the application of oil or waxes has been well-known to preserve porous gemstone materials, including jades. Since the 1980s, the impregnation treatment using artificial epoxy resins has been developed and quick diffused, due to its higher durability.

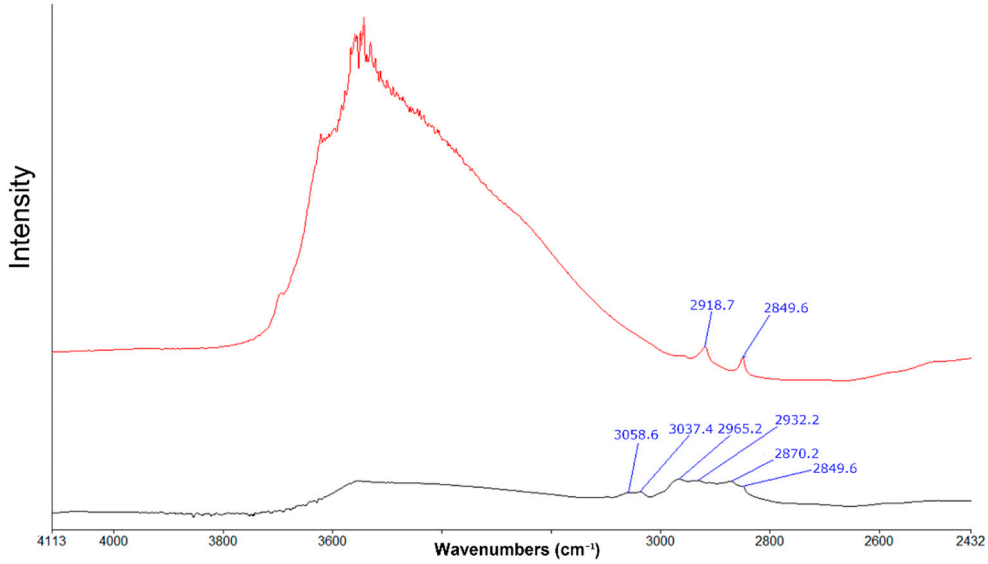

Figure 9. IR absorption spectra of two Jadeite samples: jadeite with traces of surface waxing or oiling, which can be typically correlated with polishing and cutting operation, is reported in red [156], while the black line characterizes jadeite impregnated with epoxy resin [155,156]. The range between 2500 and 3300 cm^{-1} is the most suitable for organic compound impregnation treatments detection, due to the strong absorptions correlated with the CH stretching vibrational modes [155,156]. Spectra have been acquired by Frontier FTIR spectroscope, PerkinElmer, equipped with Harrick reflection sphere, and analyzed with Spectrum Software. Data: M. Musa, GECI.

In Green Stones modern trade, the so-called "bleaching" treatment applied especially on jadeite-jade is very common. Using this two-step treatment, less attractive brownish-grayish jadeite can become whiter, by virtue of removing impurities (causing the brown and gray colors) by a chemical attack process, followed by a deep polymeric (epoxy resins) impregnation [155–157]. This procedure originates the "type B" jade [84].

Although this treatment is not common in cultural heritage or archaeological samples, substances such as oil, wax, and other materials may be used by conservators to protect the surface of an object instead of the previously used varnishes [55]. Therefore, care must be taken to determine if it is a treatment or only a conservation measure of the gems [85]. For

all these reasons, when analyzing Green Stones, taking into account current treatments can complete the characterization of the samples.

Thus, Raman and FTIR spectroscopies can be considered as complementary techniques.

4.5. The Chromophores Study and the UV-Vis/NIR Spectroscopy Application

A UV-Vis/NIR analysis is suitable for Green Stones to distinguish between natural color or treated color (Figure 10). Indeed, bleaching and dyeing treatments for modern jade materials are relatively common [84]. In particular, the dyeing procedure, usually subsequent to the "bleaching" and impregnation treatment, is a treatment able to increase the jade colors (in this case, the green is discussed, but the treatment is not limited to it), due to the addition of artificial pigments [158,159]. In gemology, the terms jade-C, when it is only dyed, and jade-B + C, when it is impregnated and dyed, are commonly accepted [84]. As per the polymer impregnation treatment discussed above, the detection of artificial or enhanced colorations for green jadeite can be evaluated for authenticity. In Figure 10, two reference absorption spectra of natural green jadeite and dyed green jadeite are reported, (a) and (b), respectively. In parallel, the spectra acquired by a gemological handheld spectroscope on the same materials have been reported below the corresponding UV-Vis Spectra (Figure 10c,d). The visible range can be considered diagnostic due to the presence of the Cr^{3+} characteristic absorptions at about 633, 657, and 692 nm corresponding to the jadeite-jade A, naturally green, or the broad absorptions between 600 and 700 nm for dyed green jadeite (jade B + C).

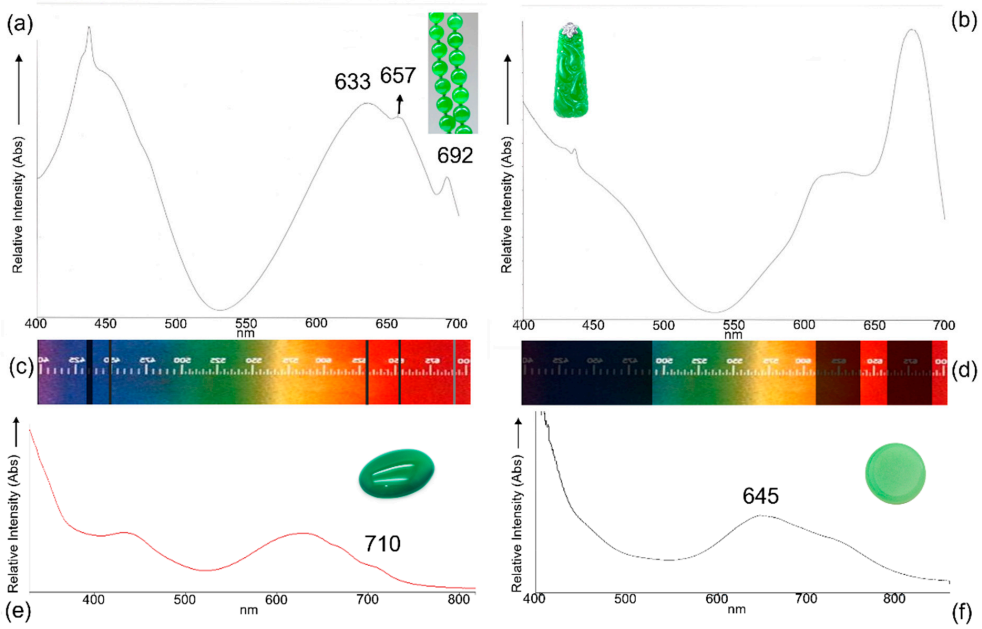

Figure 10. (**a**,**b**,**e**,**f**) UV-Vis/NIR and (**c**,**d**) gemological handheld spectroscope spectra of Green Stones. Spectra acquired by UV-Vis/NIR spectrophotometer Lambda 950, PerkinElmer, equipped with integration sphere, Spectrum Software. The two "handheld" spectra (**c**,**d**) have been reported flipped to highlight the similarities in the band absorption in correspondence to the top spectra. In particular, (**a**) Natural Imperial Green Jadeite-Jade A, the sharp absorption at about 633, 657, and 692 nm, correlated with Cr^{3+}, should be noted; (**b**) Treated Jadeite-Jade B + C, note the broadening of the bands corresponding to orange and red visible ranges (photos and spectra: M. Musa, gemological handheld spectroscope images: L. Greggio, GECI.); (**e**) Dyed Green chalcedony (Jade imitation), it is interesting to observe the absorptions in the same areas of the natural Cr^{3+} but showing characteristic broader bands, especially about 710 nm. These impregnations and modern dyeing treatments are performed using chromium-rich pigments; (**f**) Natural chrysoprase color is due to nickel-associated minerals, as shown by the characteristic UV-Vis/NIR spectrum, with the absorption centered at about 645 nm. (Data and photos: M. Musa, GIG).

Because of Green Stones massive and frequently natural porous textures, dyeing treatments are very common in the trade, not only for the jades but also applied to other gemstone materials, such as the chalcedony. By applying UV-Vis/NIR spectroscopy, as reported in Figure 10e, the identification of the Cr-rich artificial pigment results is less evident than the jadeite dyeing example. Still, it can be diagnosed because of the broader absorptions of the band at about 710 nm. Consequently, the visible range is not enough and must be expanded through the NIR. In spite of this being easily possible by UV-Vis/NIR digital spectrophotometers (whether benchtop or optical fibers portable system), the gemological handheld spectroscope does not allow the analysis beyond the visible range (400–700 nm). Moreover, the digital spectrophotometers are obviously more sensitive than the handheld gemological spectroscope. In the case of dyeing suspects, a deep OM study is mandatory: frequently, the dyed samples show characteristic colors concentrations along the fractures [84,158,160]. Similarly, the analysis of chrysoprase with natural color shows a diagnostic UV-Vis/NIR spectrum (Figure 10f), where the broad absorption correlated with nickel chromophore is visible in the range between 600 and 800 nm [106], as an asymmetric band centered at about 645 nm.

Thus, UV-Vis/NIR spectroscopy alone, or combined with gemological handheld spectroscopy (if applicable), is a suitable technique to verify the origin of the colors in gemstone materials and is particularly useful in determining the source of color for Green Stones samples.

4.6. Fluorescence Imaging

A diffused and very useful analytical technique for gemstone analysis consists of fluorescence observation. By the Wood lamp, alternative UVLW and UVSW are applied to excite the sample and the eventual fluorescence in the visible range can be directly observed or detected by digital systems. For what concerns the application on Green Stones, which usually show no or only faint fluorescence, this technique can reveal interesting information regarding the homogeneity of the sample or, eventually, surface treatments. An example of this is the chalky bluish white strong fluorescence at short wavelength of polished jadeite, treated with a new generation of polymer coating (not classical epoxy resins). This fluorescence is not consistent with the natural fluorescence behavior of jadeite, that is, none to faint white fluorescence at LW and none at SW (Table 2). In this case, Zhang [161] reported the unusual case of 10 low-quality jades cabochon samples obtained from the Guangzhou gem market. The samples showed a surface coating more similar to a film rather than a classic impregnation, identified by the authors as an organic polymeric coating. In particular, when examined with the DiamondView^{TM}, the coating fluoresced slightly blue with alternating brighter spots. Moreover, by this technique, the areas of the sample covered by the coating versus the areas where the coating had been removed were clearly evident, strongly assisting the author in the diagnosis.

It must be noted that occasionally surface coatings and/or impregnation substances can be applied for the maintenance of cultural heritage samples [162,163]. In fact, coatings are normally applied to gem materials to counterfeit or improve luster and, in some cases, provide a degree of stability [161,164,165].

For all these reasons, fluorescence imaging can be considered a complementary technique to the OM study.

The Wood lamp is a typical portable instrument and, of course, it does not require any sample preparation.

4.7. Chemical Characterization: Elemental Analyses

The final information discussed in the present review consists of the chemistry and relative analytical techniques.

For the chemical analyses of Green Stones, note the general chemical formula discussed previously in Table 3. The chemical analysis is not so significant for the phase identification, which can be easily carried out by other analytical techniques as previously discussed. On

the other hand, elemental analysis is a deeper and complementary investigation, focusing on the origin of the color (natural or due to treatment), to be combined with UV-Vis/NIR information and which is extremely useful for geographic origin determination. This last factor is a very delicate discussion point, because the origin determination can be made not on the basis of the main elements common to all gemstones belonging to the same mineral phases but on trace elements quantification. Another factor which complicates the analysis interpretation is that Green Stones are typically composed of mineral associations, as previously discussed. Moreover, due to their characteristic genetic processes, involving metamorphic alterations, differences can be detected in the chemical traces of samples coming from different points of the same veins. To bypass this issue, or at least collect reliable information for origin identification, a systematic source characterization is beneficial.

In this scenario, the first choice for elemental analysis is the ED-XRF technique, due to its non-destructive characteristics and the availability of the portable system, as previously discussed [78,79]. For example, Delgado Robles et al. [166] described the application of a portable XRF system (PXRF) for in situ analyses at the Palenque site museum. The goal of the paper was the characterization (performed with a multidisciplinary approach) of the green objects belonging to the Palenque Mayan royal burial. PXRF was helpful in tracking the origin of the minerals constituting the analyzed samples, by taking into consideration their elemental compositions, calculated from semiquantitative analyses. In fact, on the basis of the samples' chemical traces ratios, compared with references materials analyzed in the same conditions, two different sources can be identified for the samples' origin: Montagua and Verapaz. Unfortunately, a set of standards of referent materials/stones are not always available. Al Kindi [90] reported the study of several neolithic nephrite axes, discovered in Dhofar governorate (Sultanate of Oman), where the elemental characterization was performed by ED-XRF. In this second case, the data obtained for the samples have been compared by a semi-quantitative method, with the data obtained in one sample collected from the nephrite veins of Lawdar District (Yemen). Despite reporting a good correlation between the nephrite axes compositions and the reference (not only for the ratios of the main constituting elements, but also concerning zinc and potassium traces, probably correlated to secondary minerals), the relationship between the western Yemen mine and the coastal and interior Dhofar site has been only hypothesized. Anyhow, the data acquired allowed the foundations to be laid in relation to interpreting the framework of long-distance exchanges in the area, which can be expanded by further studies.

Regarding the elemental composition, two other techniques can be considered and combined in a multidisciplinary approach with standard petrographic analyses: SEM-EDS and LA-ICP-MS. With the first one, a deep study of the morphology and textures combined with chemical information at high magnification can be performed.

Considering the second technique, a spot quantitative chemical analysis is possible. It is interesting to note that with LA-ICP-MS, not only the heavier but also the lighter elements can be detected and quantified [20,81,82,167]. Both techniques can supply very important information, complementary to the ones obtained by ED-XRF. The recent (2021) paper of Zhang et al. [168] can be considered as a good example of LA-ICP-MS's potentiality for Green Stones origin determination. In fact, the authors reported the crucial origin discussion and determination of Sujiacun serpentines samples that were obtained for trace elements and rare earth elements (REE) using this technique.

Unfortunately, these two techniques are not portable and cannot be applied to all Green Stones gemstones and cultural heritage samples, due to sample preparation necessities and micro-destructive applications, respectively. For example, Manrique-Ortega et al. [169] reported during their study, for a jadeite characterization analytical dissertation for SEM-EDS analyses, that a 60 µm thick polished section was prepared from each specimen. In other cases, SEM-EDS analyses can be performed without sample preparation but with several limitations. Liu [126] reported the use of a variable pressure system to avoid the metal coating on jade materials. The chemical information in this case can be interpreted

only as semi-quantitative. Moreover, limitations correlated with the dimensions of the sample fittable in the SEM camera must also be considered [170].

Similar dimensions problems must also be considered for LA-ICP-MS; nevertheless, Golitko [171] discussed the advantages and limitations of an open-cell system applicable for samples with huge dimensions. Another application problem, as previously discussed (see Section 3.4) is related to the ablation spot dimensions, from which the materials are extracted for the analysis. Basically, the laser spot size and mass resolution need to be adjusted to produce signals of comparable intensities for standards and samples. For example, Martin et al. [172], in their study of boron and lithium isotopic distribution in different mineral phases, such as mica, pyroxenes, and serpentines, modulated ablation laser spots between 5 and 175 µm. Of course, the cited bigger dimensions are not compatible with cultural heritage applications, while they can be applied without problems on reference samples for mine characterization. Generally, when characterizing archaeological and gemstone samples, 30 to 40 µm are reported for ideal ablation crater dimensions and each sample is usually from three to five spots [171,173,174]. Typically, ablation sampling spots cannot be applied to all archaeological samples, *objets d'art*, museum samples, etc.

5. Conclusions

On the basis of the information discussed, for the identification and characterization of Green Stones, it is possible to consider the application of multidisciplinary analytical protocols (Figure 11).

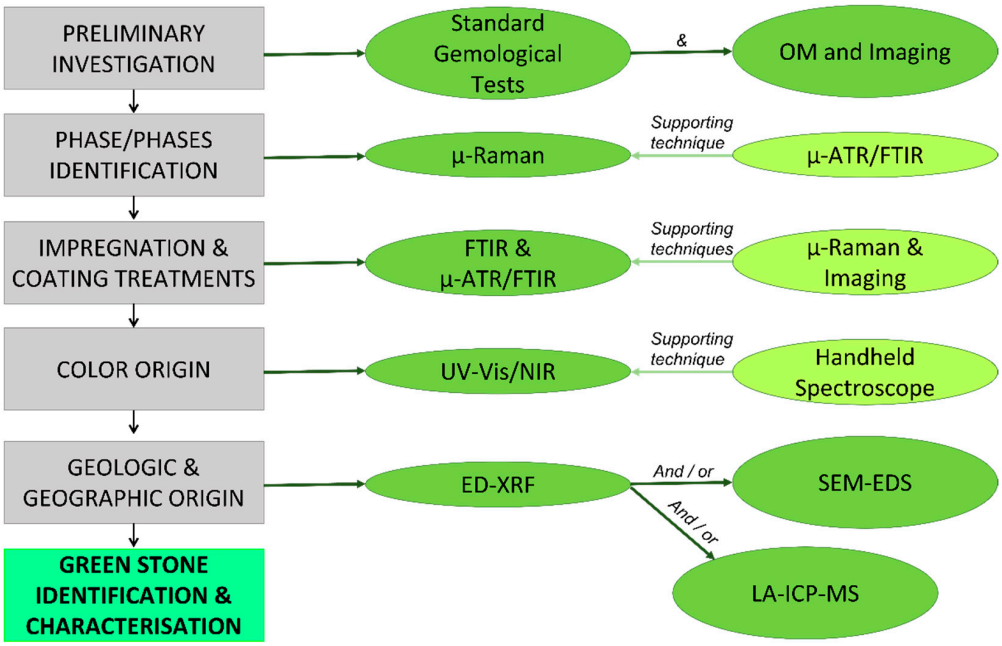

Figure 11. A summary of the multidisciplinary analytical approach applicable to the identification of Green Stones and the characterization process.

After a deep and unavoidable study by the basic gemological test, including fluorescence, plus a deep OM observation, the sample must be analyzed by spectroscopic techniques. micro-Raman spectroscopy is the best tool for the phase identification. Although identifying samples by FTIR spectroscopy is possible, the application of this second technique should be considered as complementary, especially when it is necessary to increase the information related to treatments, eventually applied to the sample.

Four complementary techniques may be considered regarding the elemental composition: the ED-XRF for a quick, easy, and "bulk" (with the previously discussed acceptation) chemical analysis; then a deeper investigation combining the gemological handheld spectroscope and UV-VIS/NIR spectrophotometer information. Using this combination, the

sample chemistry can be investigated and detailed information regarding the chromophore groups and/or transition metals becomes available, even if in traces, based on selective absorptions. The SEM-EDS technique and/or LA-ICP-MS can then be used to investigate more deeply the relationship between the chemistry and morphology/texture of the sample and eventually identify lighter and/or traces elements, not detectable by ED-XRF.

For these reasons, Green Stones are a good example to underline the importance of a multidisciplinary approach in cultural heritage studies.

Funding: This research received no external funding.

Institutional Review Board Statement: Not applicable.

Informed Consent Statement: Not applicable.

Data Availability Statement: Not applicable.

Acknowledgments: The author would like to thank the Special Issue Editors and the Applied Science Editors for assistance in enhancing the quality of the present paper, as well as the reviewers for their kind and precious work. The GIG (Gulf Institute of Gemology, Muscat, Sultanate of Oman) and all of its team is gratefully acknowledged for analytical support. Special thanks also to Lisa Greggio for her support, availability, and knowledge of Green Stones, developed during our collaboration in recent years.

Conflicts of Interest: The author declares no conflict of interest.

References

1. Wicklein, R.C.; Schell, J.W. Case Studies of Multidisciplinary Approaches to Integrating Mathematics, Science and TechnologyEducation. *J. Technol. Educ.* **1995**, *6*, 59–76. [CrossRef]
2. Taylor, G.; Spencer, S. *Social Identities, Multidisciplinary Approaches*, 1st ed.; Routledger: Abingdon, UK, 2004; pp. 1–13.
3. Lucassen, J.; Lucassen, L.; Manning, P. *Migration History in World History, Multidisciplinary Approaches*; Brill: Leiden, The Netherlands, 2010; pp. vii–viii.
4. Isurin, L.; Winford, D.; Bot, K. *Multidisciplinary Approaches to Code Switching*; John Benjamin BV: Amsterdam, The Netherlands, 2009; pp. ix–xviii.
5. Staller, J.E.; Tykot, R.H.; Benz, B.F. *Histories of Maize: Multidisciplinary Approaches to the Prehistory, Linguistics, Biogeography, Domestication, and Evolution of Maize*; Left Coast Press Inc.: Walnut Creek, CA, USA, 2009; p. 23.
6. WordReferences. Available online: https://www.wordreference.com/enit/multidisciplinary (accessed on 18 May 2022).
7. Pasquarella, C.; Balocco, C.; Pasquariello, G.; Petrone, G.; Saccani, E.; Manotti, P.; Ugolotti, M.; Palla, F.; Maggi, O.; Albertini, R. A multidisciplinary approach to the study of Cultural Heritage environments: Experience at the Palatina Library in Parma. *Sci. Total Environ.* **2015**, *536*, 557–567. [CrossRef]
8. Cardoso, I.; Macedo, M.F.; Vermeulen, F.; Corsi, C.; Santos Silva, S.; Rosado, L.; Candeias, A.; Mirao, J. A Multidisciplinary Approach to the Study of Archaeological Mortars from the Town of Ammaia in the Roman Province of Lusitania (Portugal). *Archaeometry* **2014**, *56*, 1–24. [CrossRef]
9. Berto, L.; Doria, A.; Faccio, P.; Saetta, A.; Talledo, D. Vulnerability Analysis of Built Cultural Heritage: A Multidisciplinary Approach for Studying the Palladio's Tempietto Barbaro. *Int. J. Archit. Herit.* **2017**, *1*, 773–790. [CrossRef]
10. Masciotta, M.-G.; Roque, J.C.A.; Ramos, L.F.; Lourenço, P.B. A multidisciplinary approach to assess the health state of heritage structures: The case study of the Church of Monastery of Jerónimos in Lisbon. *Constr. Build. Mater.* **2016**, *116*, 169–187. [CrossRef]
11. Jaillot, V.; Istasse, M.; Servigne, S.; Gesquière, G.; Rautenberg, M.; Lefort, I. Describing, Comparing and Analyzing Digital Urban Heritage Tools: A Methodology Designed with a Multidisciplinary Approach. *Digit. Appl. Archaeol. Cult. Herit.* **2020**, *17*, e00135. [CrossRef]
12. Vacca, G.; Fiorino, D.R.; Pili, D. A Spatial Information System (SIS) for the Architectural and Cultural Heritage of Sardinia (Italy). *ISPRS Int. J. Geo-Inf.* **2018**, *7*, 49. [CrossRef]
13. Jans, M.M.E.; Kars, H.; Nielsen-Marsh, C.M.; Smith, C.I.; Nord, A.G.; Arthur, P.; Earl, N. In Situ preservation of archaeological bone: A histological study within a multidisciplinary approach. *Archaeometry* **2002**, *44*, 343–352. [CrossRef]
14. Maritan, L.; Mazzoli, C.; Melis, E. A multidisciplinary approach to the characterization of Roman gravestones from Aquileia (Udine, Italy). *Archaeometry* **2003**, *45*, 363–374. [CrossRef]
15. Ricca, M.; Paladini, G.; Rovella, N.; Ruffolo, S.A.; Randazzo, L.; Crupi, V.; Fazio, B.; Majolino, B.; Venuti, V.; Galli, G.; et al. Archaeometric Characterisation of Decorated Pottery from the Archaeological Site of Villa dei Quintili (Rome, Italy): Preliminary Study. *Geosciences* **2019**, *9*, 172. [CrossRef]
16. Fluzin, P.; Bauvais, S.; Berranger, M.; Pagès, G.; Dillmann, P. The multidisciplinary approach (archaeology and archaeometry) to bloomsmithing activities in France: Examples of results from the last twenty years. In *The Archaeometallurgy of Iron, Recent*

Developments in Archaeological and Scientic Research; Hosek, J., Cleere, H., Mihok, L., Eds.; Institute of Archaeoology of the ASCR: Prague, Czech Republic, 2011; pp. 223–236, 311–312.
17. Agapiou, A.; Lysandrou, V.; Alexakis, D.D.; Themistocleous, K.; Cuca, B.; Argyriou, A.; Sarris, A.; Hadjimitsis, D.G. Cultural heritage management and monitoring using remote sensing data and GIS: The case study of Paphos area, Cyprus. *Comput. Environ. Urban Syst.* **2015**, *54*, 230–239. [CrossRef]
18. Belfiore, C.M.; Fichera, G.V.; La Russa, M.F.; Pezzino, A.; Ruffolo, S.A.; Galli, G.; Barca, D. A Multidisciplinary Approach for the Archaeometric Study of Pozzolanic Aggregate in Roman Mortars: The Case of Villa dei Quintili (Rome, Italy). *Archaeometry* **2015**, *57*, 269–296. [CrossRef]
19. Wagner, G.A. *Einfuhrung in Die Archaometrie*; Springer: Berlin/Heidelberg, Germany; New York, NY, USA, 2007.
20. Reindel, M.; Wagner, G.A. *New Technologies for Archaeology Multidisciplinary Investigations in Palpa and Nasca, Peru*; Springer: Berlin/Heidelberg, Germany, 2009; pp. 9–10.
21. Giannossa, L.C.; Forleo, T.; Mangone, A. The Distinctive Role of Chemical Composition in Archaeometry. The Case of Apulian Red Figure Pottery. *Appl. Sci.* **2021**, *11*, 3073. [CrossRef]
22. Columbu, S.; Sitzia, F.; Verdiani, G. Contribution of petrophysical analysis and 3D digital survey in the archaeometric investigations of the Emperor Hadrian's Baths (Tivoli, Italy). *Rend. Lincei* **2015**, *26*, 455–474. [CrossRef]
23. Jessup, R.A. *Saxon Jewellery. Faber (M0005997SH)*; Wilson Collection: London, UK, 1950; Volume 124, p. 200349501.
24. Arrhenius, B. Why the king needed his own goldsmith. *Laborativ Arkeol.* **1988**, *10–11*, 109–111.
25. Collareta, M. Oreficeria e Tecniche Orafe. In *Arti e Storia nel Medioevo. II. Del Costruire: Tecniche, Artisti, Artigiani, Committenti*; Sergi, G., Castelnuovo, E., Eds.; Giulio Enaudi: Turin, Italy, 2003; pp. 549–560.
26. Collareta, M. Storia dell'arte medievale, Intervento introduttivo. *Reti Mediev. Riv.* **2011**, *12*, 29–41.
27. Mottana, A. Italian gemology during the Renaissance: A step toward modern mineralogy. In *The Origins of Geology in Italy*; Vai, G.B., Caldwell, W.G.E., Eds.; Geological Society of America: Boulder, CO, USA, 2006; Special Paper 411; pp. 1–21.
28. Aimone, M. Nuovi dati sull'oreficeria cloisonne' in Italia tra V e VI secolo. Ricerche stilistiche, indagini tecniche, questioni cronologiche. *Archeol. Mediev.* **2011**, *XXXVIII*, 369–418.
29. Hilgner, A. Oreficeria cloisonne' nell'alto medioevo: Inquadramento cronologico sulla base degli aspetti tecnologici e dell'origine delle materie prime. In *Small Finds e Cronologia (V-IX Sec.) Esempi, Medoti e Risultati*; Pinar Gil, J., Ed.; Bradypus: Bologna, Italy, 2017; pp. 9–29.
30. CIBJO. *The Gemstone Book*; Coloured Stones Commission 2020–2021; CIBJO: London, UK, 2021.
31. Panczer, G.; Riondet, G.; Forest, L.; Krzemnicki, M.S.; Carole, D.; Faure, F. The Talisman of Charle Magne: New historical and Gemological discoveries. *Gems Gemol.* **2019**, *55*, 30–46. [CrossRef]
32. Bertelli, C. *La Corona Ferrea*; Skira: Ginevrea-Milano, Italy, 2017.
33. Riccardi, M.P.; Prosperi, L.; Tarantino, S.C.; Zema, M. Gemmology in the service of archaeometry. *EMU Notes Mineral.* **2019**, *20*, 345–366.
34. Di Martino, D.; Benati, G.; Alberti, R.; Baroni, S.; Bertelli, C.; Blumer, F.; Caselli, L.; Cattaneo, R.; Cucini, C.; D'Amico, F.; et al. The Chiaravalle Cross: Results of a multidisciplinary study. *Heritage* **2019**, *2*, 2555–2572. [CrossRef]
35. Musa, M. Gulf Institute of Gemology: An archaeometry analytical facility available "on-site". *IASA Bull.* **2021**, *26*, 45–46.
36. Martin, F.; Merigoux, H.; Zecchini, P. Reflectance InfraRed spectroscopy in Gemology. *Gems Gemol.* **1989**, *25*, 226–231. [CrossRef]
37. Fritsch, E. Gem Characterization: A Forecast of Important Techniques in the Coming Decade. *Gems Gemol.* **2006**, *42*, 90.
38. Raneri, S.; Barone, G.; Mazzoleni, P.; Bersani, D. Non-destructive spectroscopic methods for gem analysis: A short review. In Proceedings of the IMEKO TC-4 International Conference on Metrology for Archaeology and Cultural Heritage Trento, Trento, Italy, 22–24 October 2020.
39. Humphreys, E.S. How to spot a fake. *Mater. Today* **2002**, *5*, 32–37. [CrossRef]
40. Barboza, D.; Bowley, G.; Cox, A. Forging an Art Market in China. *New York Times*, 28 October 2013.
41. Barone, G.; Bersani, D.; Jehlicka, J.; Lottici, P.P.; Mazzoleni, P.; Raneri, S.; Vandenabeele, P.; Di Giacomo, C.; Larinà, G. Nondestructive investigation on the 17–18th centuries Sicilian jewelry collection at the Messina regional museum using mobile Raman equipment. *J. Raman Spectrosc.* **2015**, *46*, 989–995. [CrossRef]
42. Rudoe, J. The faking of gems in the x8th century. In *Why Fakes Matter. Essays on the Problems of Authenticity*; Jones, M., Ed.; The British Museum Press: London, UK, 1992; pp. 23–28.
43. Gordon, R. Archaeologies of Magical Gems. In *'Gems of Heaven': Recent Research on Engraved Gemstones in Late Antiquity, AD 200-600*; Entwistle, C., Adams, N., Eds.; British Museum Research Publications: London, UK, 2011; pp. 39–49.
44. Buttrey, T.V. Natter on gem collecting. Thomas hollis and some problems in the Museum Britannicum. *J. Hist. Collect.* **1990**, *2*, 219–226. [CrossRef]
45. Rudoe, J. Eighteenth and Nineteenth-Century Engraved Gems in the British Museum; Collectors and Collections from Sir Hans Sloane to Anne Hull Grundy. *Z. Kunstgesch.* **1996**, *59*, 198–213. [CrossRef]
46. Drayman-Weisser, T. From fake to fabulous: Redeeming fakes at the Walters Art Museum. *AIC Objects Spec. Group Postprints* **2007**, *14*, 90–109.
47. McClure, S.F.; Moses, T.M.; Shigley, J.E. The Geographic Origin Dilemma. *Gems Gemol.* **2019**, *37*, 457–462.
48. Gubelin Gem Lab Provenance Proof Project. Available online: https://www.provenanceproof.com/ (accessed on 25 May 2022).

49. GRS GemResearch SwissLab—Reference Collection. Available online: https://www.gemresearch.ch/research/reference-collection (accessed on 25 May 2022).
50. Krzemnicki, M.S. Origin Determination and Traceability: An Overview for Gemstones. Presented at the GemGeneva, Geneva, Swiss, SSEF Presentation. Available online: https://www.ssef.ch/presentations/ (accessed on 25 May 2022).
51. Gem Society. Available online: https://www.gemsociety.org/article/evaluating-color-hue-tone-and-saturation/ (accessed on 18 June 2022).
52. Laboratory Manual Harmonisation Committee—LMHC. *Information Sheet 0: Guidelines for Gemmological Laboratory Reports*; Version 2; LMHC: Lucerne, Switzerland, 2018.
53. Cibjo, Retailers' Reference Guide (RRG). Available online: https://www.cibjo.org/the-retailers-reference-guide/ (accessed on 20 June 2022).
54. Nickerson, D. History of the Munsell Color System and Its Scientific Application. *J. Opt. Soc. Am.* **1940**, *30*, 575–586. [CrossRef]
55. CIBJO. *The Gemmological Laboratory Book*; Gemmological Commission 2020–2021; CIBJO: London, UK, 2021.
56. GIG—Gulf Institute of Gemology. *Gemstones Identification Manual*; GIG: Muscat, Oman, 2020.
57. Sturman, D.K. A new approach to the teaching and use of the refractometer. *J. Gemmol.* **2010**, *32*, 74–89. [CrossRef]
58. Burbage, E.J.; Anderson, B.W. An analysis of the movements of shadow-edges on the refractometer in the case of biaxial gemstones. *Mineral. Mag.* **1942**, *26*, 246–253. [CrossRef]
59. Thibault, W.N. A simple dichroscope. *Am. Mineral.* **1940**, *25*, 88–90.
60. He, T. The Applications of Ultraviolet Visible Absorption Spectrum Detection Technology in Gemstone Identification. In Proceedings of the 5th International Conference on Materials Engineering for Advanced Technologies—ICMEAT, Quebec, QC, Canada, 5–6 August 2016. ISBN 978-1-60595-373-1.
61. Sinkankas, J. Contribution to history of gemology: Specific gravity—Origins and development of the hydrostatic method. *Gems Gemol.* **1986**, *157*, 156–165. [CrossRef]
62. Read, P. *Gemmology*, 2nd ed.; Routledge: London, UK, 1999; Chapter 6.
63. Koivula, J.I. Photomicrigraphy for gemologists. *Gems Gemol.* **2003**, *39*, 4–24. [CrossRef]
64. Breeding, C.M.; Shen, A.H.; Eaton-Magana, S.; Rossman, G.R.; Shigley, J.E.; Gilbertson, A. Developments in Gemstone Analysis Techniques and Instrumentation during the 2000s. *Gems Gemol.* **2010**, *46*, 241–257. [CrossRef]
65. Dietzek, B.; Cialla, D.; Schmitt, M.; Popp, J. Introduction to the Fundamentals of Raman Spectroscopy. In *Confocal Raman Microscopy*, 2nd ed.; Toporski, J., Dieing, T., Hollricher, O., Eds.; Springer: Berlin, Germany, 2018; pp. 47–67.
66. Rinaudo, C.; Croce, A.; Musa, M.; Allegrina, M. La Spettroscopia Raman come mezzo di identificazione e caratterizzazione di materiali gemmologici. *Riv. Gemmol. Ital.* **2010**, *5*, 108–112.
67. Downs, R.T.; Denton, M.B. Report on the Progress of the RRUFF Project: An Integrated Database of Raman Spectra, X-ray Diffraction, and Chemical Data for Minerals. *Gems Gemol.* **2006**, *42*, 89–90.
68. Hollricher, O. Raman Instrumentation for Confocal Raman Microscopy. In *Confocal Raman Microscopy*, 2nd ed.; Toporski, J., Dieing, T., Hollricher, O., Eds.; Springer: Berlin, Germany, 2018; pp. 69–87.
69. Frezzotti, M.L. Applicazione della Spettroscopia Raman agli studi di mineralogia e petrologia. *Plinius* **2001**, *26*, 62–73.
70. Fritsch, E.; Stockton, C.M. Infrared spectroscopy in gem identification. *Gems Gemol.* **1987**, *23*, 18–26. [CrossRef]
71. Musa, M.; Kounturaki, E. High-Tech Box: Fourier Transform Infrared Spectroscopy (FTIR). *Gulf Gemol. Mag.* **2020**, 57. Available online: https://gulfgemology.com/gulf-gemology-mag-00-special-issue/ (accessed on 13 July 2022).
72. Ochiai, S. Diffuse-Reflection Measurements. In *Introduction to Experimental Infrared Spectroscopy*; Tasumi, M., Sakamoto, A., Eds.; Wiley: Oxford, UK, 2015; pp. 169–178.
73. Griffiths, P.R.; De Haseth, J.A. microscpetroscopy and imaging. In *Fourier Infrared Spectrometry*, 2nd ed.; Wiley: Oxford, UK, 2007; pp. 303–320.
74. Zhou, D.; Lu, T.; Zhang, J. Study on the correlation between trace elements and colorimetric parameters of natural blue sapphire. *Color* **2022**, *47*, 691–696. [CrossRef]
75. Karampelas, S.; Fritsch, E.; Gauthier, J.-P.; Hainschwang, T. UV-Vis-NIR reflectance spectroscopy of natural-color saltwater cultured pearls from *Pinctada margaritifera*. *Gems Gemol.* **2011**, *47*, 31–35. [CrossRef]
76. Bernini, D.; Caucia, F.; Boiocchi, M. Application of the Vis-NIR Avaspec-2048 portable automatic spectrometer to distinguish GEM quality materials. *N. Jb. Miner. Abh.* **2009**, *185*, 281–288. [CrossRef]
77. Muhlmeister, S.; Fritsch, E.; Shigley, J.E.; Devouard, B.; Laurs, B.M. Separating natural and synthetic Rubies on the basis of trace element Chemistry. *Gems Gemol.* **1998**, *34*, 80–101. [CrossRef]
78. Brouwer, P. What is XRF. In *Theory of XRF*; PANalytical, B.V.: Almelo, The Netherlands, 2010; Chapter 2; pp. 8–9.
79. Shackley, M.S. An Introduction to X-Ray Fluorescence (XRF) Analysis in Archaeology. In *X-ray Fluorescence Spectrometry (XRF) in Geoarchaeology*; Shackley, M.S., Ed.; Springer: New York, NY, USA, 2011; pp. 12–13.
80. Goldstein, J.I.; Newbury, D.E.; Michael, J.R.; Ritchie, N.W.M.; Scott, J.H.J.; Joy, D.C. Variable Pressure Scanning Electron Microscopy (VPSEM). In *Scanning Electron Microscopy and X-ray Microanalyses*, 4th ed.; Springer: New York, NY, USA, 2018; Chapter 12; pp. 173–186.
81. Abduriyim, A.; Kitawaki, H. Application of laser ablation inductively coupled plasma mass spectrometry (LA-ICP-MS) to gemology. *Gems Gemol.* **2006**, *42*, 98–118. [CrossRef]

82. Sylvestor, P. Laser Ablation ICP-MS in the earth sciences: Current practices and outstanding issues. *Min. Ass. Can. Short Course* **2008**, *40*, 356.
83. Harlow, E.; Murphy, A.R.; Hozan, D.; De Mille, C.N.; Levinson, A.A. Pre-Columbian Jadeite axes from Antigua, West Indies: Description and possible sources. *Can. Mineral.* **2006**, *44*, 305–321. [CrossRef]
84. Laboratory Manual Harmonisation Committee—LMHC. *Information Sheet 11: Jade and Related Minerals*; Version 4; LMHC: Lucerne, Switzerland, 2011.
85. Karampelas, S.; Kiefert, L.; Bersani, D.; Vandenabeele, P. *Gems and Gemmology: An Introduction for Archaeologists, Art-Historians and Conservators*, 1st ed.; Springer: Cham, Switzerland, 2020; pp. 18–83.
86. Salviati, F. Jade, the radiance from within. In *The Asian Art Legacy*; Oljeda, A., Ed.; Casa Asia: Madrid, Spain, 2010; pp. 141–147.
87. Krzemnicki, M.S. Jade, stone of "Gods": Terms, concepts & certification. *Facette* **2012**, 8–11. Available online: https://www.ssef.ch/ssef-facette/ (accessed on 13 July 2022).
88. Middleton, A.; Freestone, I. The mineralogy and occurrence of Jade. In *Chinese Jade from the Neolithic to the Qing*; Rawson, J., Ed.; British Museum Press: London, UK, 1995; p. 413.
89. Salviati, F. Alla ricerca della pietra verde. La giada nel mondo antico. *Archeo* **1998**, *6*, 59.
90. Al Kindi, M.; Charpentier, V.; Maiorano, M.P.; Musa, M.; Pavan, A.; Heward, A.; Vosges, J.; Marchand, G.; Pickford, M. Neolithic long-distance exchanges in Southern Arabia: A supposed road for the 'Jade' axes. *J. Archaeol. Sci. Rep.* **2021**, *39*, 103116. [CrossRef]
91. Harlow, G.E.; Tsujimori, T.; Sorensen, S.S. Jadeites and Plate Tectonics. *Annu. Rev. Earth Planet. Sci.* **2014**, *43*, 105–138. [CrossRef]
92. Bakamska, A.; Abrashev, M.; Kostov, R.I. Omphacite-bearing axes from the Early Neolithic site Galabnik (Western Bulgaria): Mineral identification by Raman spectroscopy. *Rev. Bulg. Geolog. Soc.* **2018**, *79*, 51–57.
93. Bertorino, G.; Franceschelli, M.; Marchi, M.; Luglié, C.; Columbu, S. Petrographic characterization of polished stone axes from Neolithic Sardinia, archaeological implications. *Per. Miner.* **2002**, *71*, 87–100.
94. Pétrequin, P.; Errera, M.; Pétrequin, A.-M.; Allard, P. The neolithic quarries of Mont Viso, Piedmont, Italy: Initial radiocarbon dates. *Eur. J. Archaeol.* **2006**, *9*, 7–30. [CrossRef]
95. Domínguez-Bella, S.; Cassen, S.; Pétrequin, P.; Přichystal, A.; Martínez, J.; Ramos, J.; Medina, N. Aroche (huelva, andalucía): A new neolithic axehead of alpine jade in the southwest of the iberian Peninsula. *Archaeol. Anthropol. Sci.* **2016**, *8*, 205–222. [CrossRef]
96. Franz, L.; Sun, T.T.; Hanni, H.A.; De Capitani, C.; Thanasuthipitak, T.; Atichat, W. A Comparative Study of Jadeite, Omphacite and Kosmochlor Jades from Myanmar, and Suggestions for a Practical Nomenclature. *J. Gemmol.* **2014**, *34*, 210–229. [CrossRef]
97. *HKSM/FCT-2016*; Standard Methods for Testing Fei Cui for Hong Kong. The Gemmological Association of Hong Kong (Limited): Hongkong, China, 2016.
98. Gubelin, E. Maw-sit-sit: A new decorative gemstone from Burma. *Gems Gemol.* **1965**, *11*, 227–238.
99. Gubelin, E. Maw-sit-sit proves to be jade-albite. *Gems Gemol.* **1965**, *11*, 302–308. [CrossRef]
100. Manson, D.V. Recent activities in GIA's research department. *Gems Gemol.* **1979**, *16*, 217–219.
101. Hanni, H.A.; Meyer, J. Maw-sit-sit (kosmochlor-jade): A metamorphic rock with complex composition from Myanmar (Burma). In Proceedings of the 26th International Gemmological Conference, Idar-Oberstein, Germany, 27 September–3 October 1997; pp. 22–24.
102. Colombo, R.; Rinaudo, C.; Trossarelli, C. The mineralogical composition of maw-sit-sit from Myanmar. *J. Gemm.* **2000**, *27*, 87–92. [CrossRef]
103. Barrie, C. Electron backscatter diffraction investigation of length-fast chalcedony in agate: Implications for agate genesi. *Geofluids* **2012**, *13*, 32–44. [CrossRef]
104. Chauviré, B.; Rondeau, B.; Mangold, N. Near infrared signature of opal and chalcedony as a proxy for their structure and formation conditions. *Eur. J. Mineral.* **2017**, *29*, 409–421. [CrossRef]
105. Lule-Whip, C. Chromium Chalcedony from Turkey and Its Possible Archeological Connections. *Gems Gemol.* **2006**, *42*, 115.
106. Shigley, J.E.; Laurs, B.M.; Renfro, N.D. Chrysoprase and prase Opal from Haneti, central Tanzania. *Gems Gemol.* **2009**, *45*, 271–279. [CrossRef]
107. World Health Organization (WHO). 6.2 Asbestos. In *Air Quality Guidelines for Europe*, 2nd ed.; WHO Regional Publications, European Series, No. 91; World Health Organization Regional Office for Europe: Copenhagen, Denmark, 2000; Available online: http://www.euro.who.int/__data/assets/pdf_file/0005/74732/E71922.pdf (accessed on 11 March 2014).
108. Tremain, C.G. Pre-Columbian "Jade": Towards an improved identification of green colored stone in Mesoamerica. *Lithic Technol.* **2014**, *39*, 137–150. [CrossRef]
109. Gunther, B. *Tables of Gemstones identification—Bestimmungstabellen fur Edelstein, Synthesen, Imitationen*, 3rd ed.; Verlagsbuchhandlung Birgit Günther: Idar-Oberstein, Germany, 2008; p. 256.
110. Anderson, B.W. *Gem Testing*, 10th ed.; Jobbins, E.A., Ed.; Butterworth Co., Ltd.: Oxford, UK, 1990; ISBN 0-408-02320-1.
111. Liddicoat, R.T. *Handbook of Gem Identification*, 12th ed.; Gemmological Institute of America: Carlsbad, CA, USA, 1993; ISBN 0-87311-021-8.
112. Webster, R. *Gemmologists' Compendium*, 7th ed.; N.A.G. Press: London, UK, 1998.
113. Shi, G.; Wang, X.; Chu, B.; Cui, W. Jadeite Jade from Myanmar: Its texture and gemmological implications. *J. Gemmol.* **2009**, *31*, 5–8. [CrossRef]

114. Deer, W.A.; Howie, R.A.; Zussman, J. *An Introduction to the Rock-Forming Minerals*, 2nd ed.; Longman Group UK Limited: London, UK, 1992.
115. Groat, L.A.; Giuliani, G.; Stone-Sundberg, J.; Sun, Z.; Renfro, N.D.; Palke, A.C. A Review of analytical methods used in geographic origin determination of gemstones. *Gems Gemol.* **2019**, *55*, 512–535. [CrossRef]
116. Prockor, S.A. The genesis of Nephrite and emplacement of the Nephrite bearing ultramafic complexes of east sayan. *Int. Geol. Rev.* **1991**, *33*, 290–300. [CrossRef]
117. Heaney, P.J. A proposed mechanism for the growth of chalcedony. *Contrib. Mineral. Petrol.* **1993**, *115*, 66–74. [CrossRef]
118. Jenkins, A.L.; Larsen, R.A. Gemstone identification using Raman Spectroscopy. *Spectrosc* **2004**, *19*, 20–25.
119. Kiefert, L.; Karampelas, S. Use of the Raman spectrometer in gemmological laboratories: Review. *Spectrochim. Acta A Mol. Biomol. Spectrosc.* **2011**, *80*, 119–124. [CrossRef] [PubMed]
120. Schubnel, H.J.; Pinet, M.; Smith, D.C.; Lasnier, B. (IV) Spectres Raman des principales gemmes. In *La Microsonde Raman en Gemmologie*; Ruskoné, E., Ed.; Association Francaise de Gemmologie: Paris, France, 1992; pp. 18–54.
121. Rinaudo, C.; Belluso, E.; Gastaldi, D. Assessment of the use of Raman Spectroscopy for the determination of amphibole asbestos. *Mineral. Mag.* **2004**, *68*, 455–465. [CrossRef]
122. Manrique-Ortega, M.D.; Mitrani, A.; Casanova-Gonzalez, E.; Perez-Ireta, G.; Garcìa-Bucio, M.A.; Rangel-Chàvez, I.; Aguilar-Melo, V.; De Lucio, O.G.; Ruvalcaba-Sil, J.L.; Sugiyama, N.; et al. Material study of green stone artifacts from a Teotihuacan complex. *Mater. Manuf.* **2020**, *35*, 1431–1445. [CrossRef]
123. Hernandez-Murillo, C.; Garcìa-Pedra, S.; Alfaro-Còrdoba, M.; Fernandez-Esquivel, P.; Ménager, M.; Montero, M.L. Influence of surface roughness on the spectroscopic characterization of jadeite and greenstones archaeological artifacts: The axe-god pendants case study. *Spectrochim. Acta A Mol. Biomol. Spectrosc.* **2022**, *267*, 120508. [CrossRef]
124. Rinaudo, C.; Allegrina, M.; Fornero, E.; Musa, M.; Croce, A.; Bellis, D. Micro-Raman spectroscopy and VP-SEM/EDS applied to identification of mineral particles and fibres in histological sections. *J. Raman Spectrosc.* **2010**, *41*, 27–32. [CrossRef]
125. Rinaudo, C.; Gastaldi, D.; Belluso, E. Characterization of Chrysotile, Antigorite and Lizardite by FT-Raman Spectroscopy. *Can. Mineral.* **2003**, *41*, 883–890. [CrossRef]
126. Liu, S.I.; Ouyang, C.M.; Ng, F.Y. The application of VPSEM-Raman coupled system in studying Fei Cui. In Proceedings of the 34th International Gemmological Conference IGC, Vilnius, Lithuania, 26–30 August 2015.
127. RRUFF Kosmochlor Reference N. R120015. Available online: https://rruff.info/kosmochlor/display=default (accessed on 13 June 2022).
128. RRUFF Chromite Reference N. R110060. Available online: https://rruff.info/chromite/R110060 (accessed on 19 June 2022).
129. RRUFF Eckermannite Reference N. R060320. Available online: https://rruff.info/eckermannite/display=default (accessed on 13 June 2022).
130. Goryainov, S.V.; Smirnov, M.B. Raman spectra and lattice-dynamical calculations of natrolite. *Eur. J. Mineral.* **2001**, *13*, 507–519. [CrossRef]
131. Perraki, M.; Karipi, S.; Rigopoulos, I.; Tsikouras, B.; Pomonis, P.; Hatzipanagiotou, K. Grossular/Hydrogrossular in rodingite from Othrys Ophiolite, (central Greece): Raman spectroscopy as a tool to distinguish it from Vesuvianite. In Proceedings of the XIX CBGA Congress, Thessaloniki, Greece, 23–26 September 2010; Scientific Annals, School of Geology, Aristotle University of Thessaloniki Special Volume. Volume 99, pp. 317–322.
132. Butek, J.; Spisiak, J.; Milovska, S. Garnet-Vesuvianite equilibrium in Rodingite from Dobsina (Western Carpathians). *Minerals* **2021**, *11*, 189. [CrossRef]
133. Huang, E.; Chen, C.H.; Huang, T.; Lin, E.H.; Xu, J.A. Raman spectroscopic characteristics of Mg-Fe-Ca pyroxenes. *Am. Miner.* **2000**, *85*, 473–479. [CrossRef]
134. Katerinopoulou, A.; Musso, M.; Amthauer, G. A Raman spectroscopic study of the phase transition in omphacite. *Vibr. Spectr.* **2008**, *48*, 163–167. [CrossRef]
135. RRUFF Pumpellyite Reference N. R120172. Available online: https://rruff.info/pumpellyite/display=default/R120172 (accessed on 13 June 2022).
136. Schmidt, P.; Bellot-Gurlet, L.; Lea, V.; Sciau, P. Moganite detection in silica rocks using Raman and infrared spectroscopy. *Eur. J. Mineral.* **2013**, *25*, 797–805. [CrossRef]
137. Gotze, J.; Nasdala, L.; Kleeberg, R.; Wenzel, M. Occurrence and distribution of "Moganite" in agate/chalcedony: A combined micro-Raman, Rietveld, and cathodoluminescence study. *Contrib. Mineral. Petrol.* **1998**, *133*, 96–105. [CrossRef]
138. Rossetti, P.; Ferrero, S. The Zn-Pb deposits of Casario (Ligurian Alps, NW Italy): Late Palaeozoic sedimentary-exhalative bodies affected by the alpine metamorphism. *Geodin. Acta* **2008**, *21*, 117–137. [CrossRef]
139. Gendron, F.; Smith, D.C.; Masson, P.; Rodríguez Martínezd, M.C.; Ortiz Ceballose, P. Portable Raman verification and quantification of jade in Olmec ceremonial axes from El Manatí, Veracruz, Mexico. *J. Raman Spectrosc.* **2017**, *48*, 1618–1632. [CrossRef]
140. Zhao, H.X.; Li, Q.H.; Liu, S.; Hub, Y.Q.; Gana, F.X. Nondestructive analysis of jade artifacts from the Cemetery of the Ying State in Henan Province, China using confocal Raman microspectroscopy and portable X-ray fluorescence spectroscopy. *J. Raman Spectrosc.* **2014**, *45*, 173–178. [CrossRef]
141. Shurvella, H.F.; Rintoul, L.; Fredericks, P.M. Infrared and Raman spectra of jade and jade minerals. *Int. J. Veh. Saf.* **2001**, *5*. Available online: http://www.irdg.org/the-infrared-and-raman-discussion-group/ijvs/ijvs-volume-5-edition-5/infrared-and-raman-spectra-of-jade-and-jade-minerals/ (accessed on 13 July 2022).

142. Coccato, A.; Karampelas, S.; Worle, M.; Van Willingen, S.; Petrequin, P. Gem Quality and Archeological Green "Jadeite Jade" vs "Omphacite Jade": A Multi-Method Study. *J. Raman Spectrosc.* **2014**, *45*, 1260–1265. [CrossRef]
143. RRUFF Jadeite Reference N. R050220. Available online: https://rruff.info/jadeite/display=default/R050220 (accessed on 13 June 2022).
144. RRUFF Actinolite Reference N. R040063. Available online: https://rruff.info/actinolite/display=default/R040063 (accessed on 13 June 2022).
145. RRUFF Tremolite Reference N. R050498. Available online: https://rruff.info/tremolite/display=default/R050498 (accessed on 19 June 2022).
146. Fritsch, E.; Balan, E.; Petit, S.; Juillot, F. Structural, textural, and chemical controls on the OH stretching vibrations in serpentine-group minerals. *Eur. J. Mineral.* **2021**, *33*, 447–462. [CrossRef]
147. RRUFF Antigorite Reference N. R070228. Available online: https://rruff.info/antigorite/display=default (accessed on 13 June 2022).
148. Bosch-Reig, F.; Gimeno-Adelantado, J.V.; Bosch-Mossi, F.; Doménech-Carbó, A. Quantification of minerals from ATR-FTIR spectra with spectral interferences using the MRC method. *Spectrochim. Acta A Mol. Biomol. Spectrosc.* **2017**, *181*, 7–12. [CrossRef]
149. Ucbas, Y.; Bozkurt, V.; Bilir, K.; Ipek, H. Concentration of chromite by means of magnetic carrier using sodium oleate and other reagents. *Physicochem. Probl. Miner. Process.* **2014**, *50*, 767–782.
150. Kobayashi, S.; Shoji, T. Infrared analysis of the grossular-hydrogrossular series. *Mineral. J.* **1983**, *11*, 331–343. [CrossRef]
151. RRUFF Vesuvianite Reference N. R050056. Available online: https://rruff.info/vesuvianite/display=default/R050056 (accessed on 13 June 2022).
152. RRUFF Diopside Reference N. R040009. Available online: https://rruff.info/diopside/display=default/R040009 (accessed on 13 June 2022).
153. RRUFF Pumpellyite Reference N. R070130. Available online: https://rruff.info/tags=101/R070130 (accessed on 13 June 2022).
154. RRUFF Quartz Reference N. R040031. Available online: https://rruff.info/quartz/display=default/R040031 (accessed on 13 June 2022).
155. Quek, P.L.; Tan, T.L. Identification of B Jade by diffuse reflectance infrared Fourier transform (DRIFT) spectroscopy. *J. Gemmol.* **1997**, *25*, 417–427. [CrossRef]
156. Fritsch, E.; Wu, S.-T.T.; Moses, T.; McClure, S.F.; Moon, M. Identification of bleached and polymer-impregnated Jadeite. *Gems Gemol.* **1992**, *28*, 176–187. [CrossRef]
157. Bersani, D.; Lottici, P.P. Applications of Raman spectroscopy to gemology. *Anal. Bioanal. Chem.* **2010**, *397*, 2631–2646. [CrossRef]
158. Hand, D. Dyed and Natural Green Jadeite. *Gems Gemol.* **2015**, *51*, 316–317.
159. Scarani, A.; Åström, M. Gemological applications of UV-Vis-NIR spectroscopy. *Riv. Ital. Gemmol.* **2017**, *7*, 1–9.
160. Tai-An Lai, L.; Tai-An, L. Dyed green marble imitating jadeite. *Gems Gemol.* **2014**, *50*, 310–311.
161. Zhang, J.; Lu, T.; Chen, H. Gemological characteristics of coated Jadeite Jade. *Gems Gemol.* **2013**, *49*, 246–251. [CrossRef]
162. Zhao, J.; Li, W.; Luo, H.; Miao, J. Research on protection of the architectural glazed ceramics in the Palace Museum, Beijing. *J. Cult. Herit.* **2010**, *11*, 279–287. [CrossRef]
163. Re, G.; Croce, A.; D'Angelo, D.; Marchese, L.; Rinaudo, C.; Gatti, G. Application of nano-coating technology for the protection of natural lapideous materials. *Surf. Coat. Technol.* **2022**, *441*, 128507. [CrossRef]
164. Tai-An Lai, L. Polymer-Coated Serpentine. *Gems Gemol.* **2016**, *52*, 165.
165. O'Bannon, E.; Williams, Q. Coated lawsonite pseudomorphs presented as chromian lawsonite. *Gems Gemol.* **2014**, *50*, 307–309.
166. Delgado Robles, A.A.; Ruvalcaba Sil, J.L.; Claes, P.; Manrique Ortega, M.D.; Casanova González, E.; Maynez Rojas, M.A.; Cuevas García, M.; García Castillo, S. Non-destructive in situ spectroscopic analysis of greenstone objects from royal burial offerings of the Mayan site of Palenque, Mexico. *Herit. Sci.* **2015**, *3*, 20. [CrossRef]
167. Diella, V.; Bocchio, R.; Caucia, F.; Marinoni, N.; Langone, A.; Possenti, E. New Insights for Gem-Quality Mn-Bearing Diopside-Omphacite, Violane Variety, from Saint Marcel (Val D'Aosta, Italy): Its Trace Elements and Spectroscopic Characterization. *Minerals* **2021**, *11*, 171. [CrossRef]
168. Zhang, B.S.; Wu, X.T.; Sun, Y.F.; Ritchey, M.; Fan, A.C.; Zhang, Y.Y.; Yu, G.; Song, Y.B. Complex raw materials and the supply system mineralogical and geochemical study of the jade artefact of the Longshan culture (2400–2000 BCE) from Sujiacun site in coastal Shandong, China. *Archaeometry* **2021**, *63*, 1–18. [CrossRef]
169. Manrique-Ortega, M.D.; Mitrani, A.; Casanova-González, E.; Jiménez-Galindo, L.A.; Ruvalcaba-Sil, J.L. Methodology for the non–destructive characterization of jadeite-jade for archaeological studies. *Spectrochim. Acta A Mol. Biomol. Spectrosc.* **2019**, *217*, 294–309. [CrossRef] [PubMed]
170. Mereuta, P.; Costantinescu, B.; Cristea-Stan, D.; Serbanescu, D. SEM-EDS as investigation tool for archaeological artifacts—The case of nephrite adornments. *Rom. Rep. Phys.* **2019**, *71*, 802.
171. Golitko, M. Introduction to Solid Sampling Strategies. In *Recent Advances in Laser Ablation ICP-MS for Archaeology*; Dussubieux, L., Golitko, M., Gratuze, B., Eds.; Springer: New York, NY, USA, 2016; pp. 23–90.
172. Martin, C.; Ponzevera, E.; Harlow, G. In situ lithium and boron isotope determinations in mica, pyroxene, and serpentine by LA-MC-ICP-MS. *Chem. Geol.* **2015**, *412*, 107–116. [CrossRef]

173. Barca, D.; De Francesco, A.M.; Crisci, G.M.; Tozzi, C. Provenance of obsidian artifacts from site of Colle Cera, Italy, by LA-ICP-MS method. *Period. Mineral.* **2008**, *77*, 41–52.
174. Wang, H.A.O.; Krzemnicki, M.S.; Chalain, J.P.; Lefévre, P.; Zhou, W.; Cartier, L.E. Simoultaneous high sensitivity trace elements and isotopic analysis of gemstones using laser ablation inductively coupled plasma time-of-flight mass spectrometry. *J. Gemmol.* **2016**, *35*, 212–223. [CrossRef]